A DROSOPHILA MODEL OF FRONTOTEMPORAL DEMENTIA (FTD) BASED ON C9ORF72 HEXANUCLEOTIDE REPEAT EXPANSION

by

Christi Williams

A Thesis Submitted to the Faculty of the

DEPARTMENT OF MOLECULAR AND CELLULAR BIOLOGY

In Partial Fulfillment of the Requirements

For the Degree of

MASTERS OF MOLECULAR AND CELLULAR BIOLOGY

In the Graduate College

THE UNIVERSITY OF ARIZONA

2022

THE UNIVERSITY OF ARIZONA
GRADUATE COLLEGE

As members of the Master's Committee, we certify that we have read the thesis prepared by: Christi Williams
titled: A DROSOPHILA MODEL OF FRONTOTEMPORAL DEMENTIA (FTD) BASED ON C9ORF72 HEXANUCLEOTIDE REPEAT EXPANSION

and recommend that it be accepted as fulfilling the thesis requirement for the Master's Degree.

Frans E. Tax
Frans E. Tax — Date: Aug 29, 2022

George Sutphin — Date: Aug 29, 2022

_____ Date: _____

_____ Date: _____

Final approval and acceptance of this thesis is contingent upon the candidate's submission of the final copies of the thesis to the Graduate College.

I hereby certify that I have read this thesis prepared under my direction and recommend that it be accepted as fulfilling the Master's requirement.

Daniela Zarnescu — Date: Aug 29, 2022
Molecular and Cellular Biology Department

Table of contents

Abstract

Frontotemporal dementia (**FTD**) is a neurodegenerative disorder characterized by a spectrum of symptoms such as loss of intellectual functions, including memory problems, impaired reasoning, abstract thinking, executive function, that can severely impact daily living activities. Frontotemporal lobar degeneration (**FTDL**) leads to a diverse group of conditions that are hallmarked by atrophy in the prefrontal and anterior temporal cortices. FTD is substantially less common than Alzheimer's disease, but still greatly impacts individual lives leading to high socioeconomic costs to treat. This specialized level of care is valued at $244 billion, but its costs extend to the family caregivers' who have an increased risk for emotional distress and negative physical and mental outcomes. Additionally, the overall incidence of cases of FTD is expected to increase, as our aging population is expected to grow by 2030 to include 1 in 5 Americans 65 years old and over.

Approximately, 43% of FTD patients have a family history related to dementia or associated neurodegenerative diseases, with up to 27% of individuals carrying an autosomal dominant mutation. When examining the subsets of familial FTD cases, mutations in three genes, microtubule-associated protein tau (**MAPT**), progranulin (**GRN**), and C9orf72, are prominent. The overarching hypothesis for this project is that overexpression of C9orf72 hexanucleotide repeat expansions (HREs) in RNA and/or dipeptide repeats (DPRs) in the encoded proteins in mushroom body neurons cause FTD like phenotypes in *Drosophila*.

The present findings in this study show that overexpression of C9orf72 hexanucleotide repeat expansions (HREs) and DPRs in Drosophila MBs causes FTD like phenotypes. Sleep studies revealed that young flies expressing RNA only HREs exhibited greater sleepiness, while polyGR DPR flies displayed sleep changes later in their lifespan. Old (60 day) RNA only HRE expressing males showed sleep fragmentation while female flies exhibited greater sleepiness. Y-Maze assays uncovered that both RNA only HREs and polyGR DPRs caused increased locomotion rather than working memory deficits, as expected. This finding indicates possible hyperactivity in C9orf72 hexanucleotide repeat expansion flies through an increase in movement at both young and old age points. Morphological studies showed a profound, age dependent axonal thinning. In summary, this study shows that both C9orf72 HRE and DPR expressing flies exhibit sleep dysregulation, hyperactivity, and MB lobe thinning changes that could be examined closer to determine the underlying mechanisms of disease and provide further information on the genetic pathways and cellular mechanisms behind C9orf72 induced FTD.

A *Drosophila* Model of Frontotemporal Dementia (FTD) Based on C9orf72 Hexanucleotide Repeat Expansion

Introduction

FTD disease description and statistics

FTD is the most widespread cause of early onset dementia that impacts an estimated 20,000 to 50,000 people in the United States (Hogan et al., 2002). FTD is a progressive neurodegenerative disease that leads to death within 3-5 years of symptom onset (Rascovsky et al., 2011b). Clinically, FTD presents as a heterogenous neurodegenerative disease with progressive alterations in behavior including sleep, personality, and/or language (Neary et al., 1998). Pathological studies on post-mortem brain tissue of FTD patients uncovered brain atrophy in the frontal and temporal lobes (Neary *et al.*, 1998).

FTD disease clinical characterization

Based upon its heterogeneous features, FTD can further be classified into three major clinical types, including a behavioral variant (bvFTD), and two forms of primary progressive aphasia (PPA) known as, non-fluent (nfvPPA) and semantic variant (svPPA) (McKhann et al., 2001). The rationale behind establishing subdivisions of FTD is to discover therapeutics that can target the diverse pathogenic process for a more specialized treatment, which is currently limited to speech, physical, or occupational therapy and psychiatric support. Interestingly, as the disease progresses these phenotypes often converge, further complicating their treatment plan. Unsurprisingly, the complexity of FTD clinical neuropathology is varied among affected individuals (A. et al., 2007). Several studies on FTD have shown that the most common overlapping pathology comprises neuronal cytoplasmic inclusions (NCI) in the superficial layers of the neocortex that are immunoreactive for ubiquitin (Trojanowski and Dickson, 2001). In addition, some cases of FTD are characterized by the accumulation of small spindle-shaped structures found within dendrites, known as argyrophilic grains (Braak and Braak, 1987). Regardless of these differences at the cellular level, a consistent feature of FTD disease presentation is the degeneration of the frontal and temporal cerebral lobes known as frontotemporal lobar degeneration (FTLD) (Neary *et al.*, 1998).

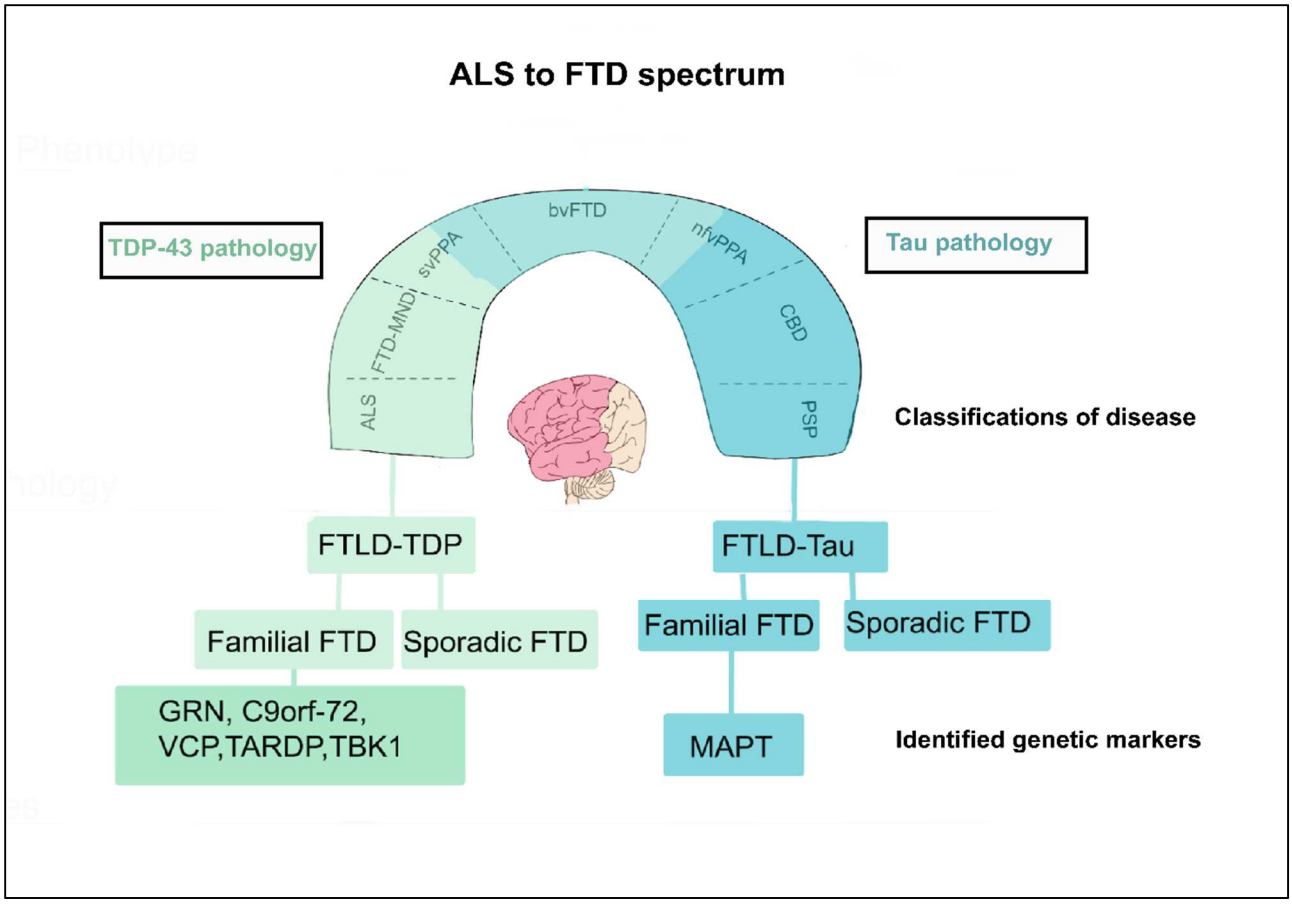

Figure 1. ALS and FTD disease pathology share common underlying genetic mutations that lie on a spectrum of clinical manifestations of different disease symptoms. This spectrum allows clinical practitioners to classify these hallmark features into clinical subtypes, including behavioral variant (bvFTD), and two forms of primary progressive aphasia (PPA) known as, non-fluent (nfvPPA) and its semantic variant (svPPA) (Trojanowski and Dickson, 2001).

Genetic basis of FTD

Evidence for an underlying genetic component of FTD is supported by studies identifying several gene mutations that have been uncovered as causative factors for the disease. Approximately 10-20% of all FTD patients exhibit an autosomal dominant mode of inheritance with mutations in genes encoding progranulin (GRN), the microtubule associated protein tau (MAPT), and a hexanucleotide repeat expansion located on chromosome 9p21 (C9orf72) as a main causative component of FTD diagnosis (Rohrer et al., 2009); (Mackenzie et al., 2011). Each mutation was found to lead to specific changes in the patients' neuropathology. For example, the PGRN mutations were found to cause cerebral atrophy that tended to be most prominent in the frontal lobes in 13 clinical cases of FTD (Baker et al., 2006). Additionally, shrinking and loss of pigmentation in the caudate nucleus and loss of pyramidal neurons of the hippocampus were linked with PGRN mutations (Baker *et al.*, 2006). MAPT mutations led to the presence of distinct atrophy patterns in the hippocampus, amygdala, temporal cortex, insula, and the orbitofrontal cortex (Young et al., 2021). Lastly, a recent study utilizing magnetic resonance

imaging found extensive thinning of the frontal, temporal, and parietal cortices in FTD patients with C9orf72 mutations (Mahoney et al., 2012). A crucial parameter for measuring changes in neuroanatomy for FTD cases is measuring brain atrophy through hemispheric asymmetry, where the left and right asymmetry ratio is derived by dividing the left hemispheric volume by the right hemispheric volume (Lehmann et al., 2010). Further studies used this neuroimaging methodology in C9orf72 patients and found that they were significantly more symmetrical in brain atrophy than the patients harboring GRN mutations and found significantly less temporal lobe involvement than the MAPT mutations (Mahoney *et al.*, 2012). These gene mutations do not contribute to one confounding symptom, but to an overall spectrum, where GRN mutations appear to associate with cases displaying asymmetrical brain atrophy patterns (Seltman and Matthews, 2012). In contrast, C9orf72 and MAPT mutations appear to be associated with syndromes displaying symmetrical atrophy patterns (Seltman and Matthews, 2012). Although the majority of FTD cases are sporadic, up to 41.8% of patients' blood samples were pooled from a cohort of 225 cases of FTD that have some family history of FTD (Wood et al., 2013). Interestingly, only 10.2% of patients with a family history of FTD had distinct autosomal dominant mutations in of MAPT, GRN, and C9orf72 (Wood *et al.*, 2013). Although the cases of specific autosomal dominant mutant inheritance are low, this gives researchers a clear understanding of how these mutations impact changes in neuroanatomy and cellular pathology.

C9orf72 in ALS/FTD

Mutations in C9orf72 recently emerged as the most frequent cause of FTD and ALS; before 2011 this gene and its protein were completely unknown (Mackenzie *et al.*, 2011). Numerous individuals have been noted with autosomal-dominant FTD and ALS, both genetically linked to chromosome 9p21 where C9orf72 is cytogenetically located. Genomic studies have reported a large hexanucleotide (G_4C_2) repeat expansion in the noncoding region, within the first intron of C9orf72 (Mackenzie *et al.*, 2011); (Renton et al., 2011); (Renton *et al.*, 2011).

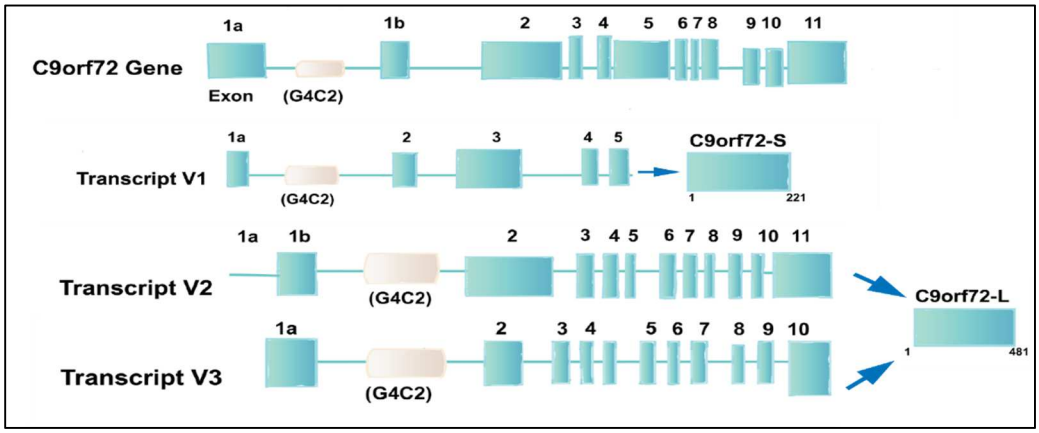

Figure 2. The human chromosome 9 open reading frame 72 (C9orf72) locus includes two non-coding exons 1b and 1a that are fused to coding exons 2 through 11 (Mackenzie *et al.*, 2011). The C9orf72 gene is transcribed into three primary transcripts (V1, V2, and V3), which yield two protein isoforms (C9orf72-S(C9-S) and C9orf72-L(C9-L). V1 is a brief transcript including non-

coding exon 1a and exons 2-5 as the coding sequence. V2 shares exons 2-11 as the coding sequence and includes non-coding exons 1b or 1a. When alternative splicing occurs, these three RNA variants result in the production of two different isoforms: the 222 amino acid isoform C9orf72-S protein encoded by V1, while the 481 isoform results in C9orf72-L protein encoded by V2 and V3 (Renton *et al.*, 2011); (Mackenzie *et al.*, 2011). Notably, the G4C2 hexanucleotide repeat mutation is (Mackenzie *et al.*, 2011). The length of this G4C2 repeat is linked to critical neurodegenerative diseases such as FTD and ALS.

Analysis of clinical studies uncovered that C9orf72 repeat expansions are the most common genetic abnormality in both familial FTD cases (11.7%) and ALS (23.5%) (Mackenzie *et al.*, 2011). Repeat expansions are associate with numerous fatal familial neurodegenerative diseases including, Alzheimer's disease (AD), sporadic Creutzfeldt-Jakob disease, and Huntington disease-like syndrome (Beck et al., 2013); (Renton *et al.*, 2011).Using a modified Southern Blotting protocol, researchers identified large C9orf72 hexanucleotide repeat expansions in six neurodegenerative disease UK cohorts including FTLD, ALS, AD, sporadic Creutzfeldt-Jakob disease, Huntington disease-like syndrome, and other nonspecific neurodegenerative disease syndromes (Beck *et al.*, 2013).This study further supports that C9orf72 mutations are indeed on a disease spectrum for FTD/ALS cases. Next, researchers found the number of hexanucleotide repeats in ALS and FTD cases correlated. Interestingly, the greater number of repeats is not a direct link to the severity of FTD/ALS symptoms. In a study with 900 healthy controls and 315 C9orf72 homozygous mutation carriers, the estimated number of (G_4C_2) repeats ranged from 700 to 1600 (Mackenzie *et al.*, 2011). In this same study, analysis of DNA from lymphoblast cell lines deduced that a healthy range of (G_4C_2) repeats ranged from 2-23 units, whereas an estimated repeat length of 700-1600 units correlated with FTD/ALS. The number of repeats was estimated using a Southern blotting technique where the average number of (G_4C_2) repeats in controls was only 2, whereas the number of repeats was greater than 800 in carriers of the C9orf72 mutation (Mackenzie *et al.*, 2011); (Smith and Shaw, 2013). These novel findings highlight the importance of C9orf72 hexanucleotide repeat expansion in neurodegenerative diseases.

By providing insight into which cellular and molecular mechanisms or combination thereof are the cause of C9ALS/FTD, we can better understand the disease mechanism to tailor appropriate clinical treatments. The exact disease mechanism behind C9orf72-induced ALS/FTD is still unclear; however, three mechanisms have been proposed. First, a loss of function mechanism could result from reduction in C9orf72 protein levels. A study examining the prevalence of FTD/ALS cases found that intermediate (G_4C_2) repeats (7-24 units) are associated with reduction in C9orf72 transcriptional activity with increasing number of normal repeat units (van der Zee et al., 2013). The genomic structure of the haplotype itself might lead to the repeat being unstable, resulting in many expansion events on a predisposing haplotype from the 3 C9orf72 transcripts (van der Zee *et al.*, 2013); (Beck *et al.*, 2013). Second, a toxic gain of function might result from repeat RNA aggregating and sequestering vital RNA binding proteins or other factors. Lastly, dipeptide repeat protein (DPR) species generation via repeat associated non-AUG (RAN) translation could cause a toxic gain of function (Gijselinck et al., 2012); (Mackenzie *et al.*, 2011); (Renton *et al.*, 2011).

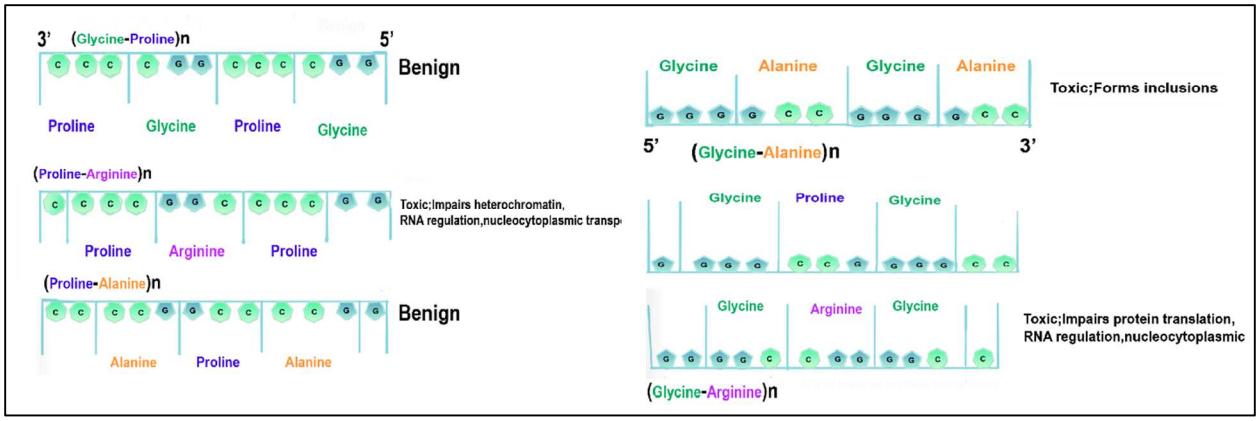

Figure 3. The exact disease mechanism behind C9orf72 induced FTD is still unclear, however, three mechanisms have been proposed including a gain of function mechanism in which RNA produces five toxic dipeptide repeat proteins (DPR) (Gijselinck *et al.*, 2012); (Mackenzie *et al.*, 2011). Each of these mechanisms result in a different disease phenotype based on their combinations and influences on FTD pathogenesis.

Current Models for underlying C9orf72 dependent FTD

To better understand the consequences of C9orf72 haploinsufficiency on FTD, various loss of function *in vivo* models have been constructed. For example, zebrafish and *Caenorhabditis elegans* loss of function models illustrated locomotor phenotypes and motor neuron degeneration (Therrien et al., 2013); (Ciura et al., 2013). This further validates that C9orf72 is a spectrum disorder for both FTD and ALS phenotypes. The C9orf72 knock-out (KO) mouse models elicit different phenotypes that did not mimic FTD-ALS disease symptoms (Simone et al., 2018); (Braems et al., 2020). One such study found that C9orf72 heterozygous and homozygous KO mice displayed no neurodegeneration and motor deficits, while complete deletion of C9orf72 led to autoimmune disorders and reduced survival (Koppers et al., 2015). Interestingly, deficits in early social recognition were found in another C9orf72 knockout model showing researchers that a deficiency in C9orf72 expression is not the sole trigger of neurodegeneration in FTD-ALS, but its exact contribution is not clear (Jiang et al., 2016). A research group investigated whether C9orf72 deficiencies were dose-dependent and found that C9 knock-out male mice displayed a decrease in latency to fall under a rotarod motor coordination (Shao et al., 2019). This leads researchers to speculate that when C9orf72 is knocked down, there is a sensitive dose-dependent response that can induce neurodegeneration or motor defects. Secondly, C9orf72 gain of function models have been developed and have had their own challenges with recapitulating the complex disease. When overexpressing the hexanucleotide repeat expansion in mice through viral delivery, both FTD and ALS histopathology and behavioral modifications were uncovered (Herranz-Martin et al., 2017); (Todd et al., 2020). In stark contrast, bacterial artificial chromosome transgenic mice displayed RNA foci formation and DPR inclusions, but neurodegeneration was rare or inconsistent (Peters et al., 2015); (Liu et al., 2016). Altogether, the gain of function model shows that, by itself, the gain of function mechanism is not sufficient in recapitulating FTD phenotypes.

Lastly, a knock in rat model was employed to demonstrate the need of combining both loss of function and gain of function mechanisms for an appropriate FTD model. Eighty (G_4C_2) repeats with flanking fragments of human exons 1a and 1b were introduced to the rat C9orf72 locus, resulting in a 40% decrease in protein expression in the brain and spinal cord (Dong et al., 2020). This study suggests that motor defects in the knock in rats may result from neurotoxicity caused by the C9orf72 hexanucleotide repeat expansion leading to a reduction in the protein expression levels. In line with this result, two other mouse studies have shown that the combination of gain of function mechanisms on top of the additional loss of function mechanism is sufficient to cause the development of FTD phenotypes in mice (Shao *et al.*, 2019); (Zhu et al., 2020). Taken together, these studies show the need for employing models of C9orf72 that can appropriately mimic repeat-dependent gain of toxicity that results in a reduction of protein expression.

In this thesis, I describe the development and characterization of a *Drosophila* model of FTD based on C9orf72 expression in mushroom body neurons, a circuit involved in learning and memory and other behaviors such as sleep. This model is expected to provide further information on the genetic pathways and cellular mechanisms underlying C9orf72 induced FTD.

Methods

Drosophila Genetics

Drosophila Genetic Constructs

Genotype	Source
w^{1118}; attP40	Generated in lab by Elise Munoz from w^{1118} and yv; attP40
w^{1118}; UAS (G4C2) 3X attP40	Bloomington Stock Center (reported in Mizielinska et al, 2014)

w^{1118}; UAS (G4C2) 108X RO attP40	Bloomington Stock Center (reported in Mizielinska et al, 2014)
w^{1118}; UAS PolyGR 100X attP40	Bloomington Stock Center (reported in Mizielinska et al, 2014)
Split Gal4 SS01276	Yoshi Aso (reported in Aso et al, 2016)

Table 1. Transgenic lines used to generate a *Drosophila* model of FTD

FTD was tested by expressing various C9 constructs in the mushroom bodies using the GAL4-UAS bipartite expression system. The Split GAL4 driver SS01276 was used to drive expression of individual transgenes (see Table 1) in MB neurons. w^{1118}; attP40 was used as a genetic background control. Individual replicates were set-up as bottle crosses using 25 Split GAL4 driver, SS01276 virgin females where two halves of the GAL4 protein are expressed under two different tissue specific promoters. Together both promoters result in expression of **α**/**β** and **γ** neurons in the MB (Aso et al., 2014). Crossing 25 virgin female Split GAL4 driver and 15 males of appropriate C9orf72 hexanucleotide repeat genotypes reported in (Mizielinska et al, 2014) resulted in adults expressing either the 108X RNA only HRE construct or the 100X polyGR construct that represent a fly model C9orf72 in which we could test clinically relevant FTD phenotypes.

Adult fly aging

Newly eclosed virgin male and female progeny were collected and maintained on 3 ml Zarnescu Lab cornmeal-molasses fly media vials purchased from the UofA media facility at 25°C with 25-50% humidity. Media was refreshed weekly until flies were used for various behavioral assays. The day that the flies were collected was considered day 1 of their adult life. Mushroom body morphology and behavioral assays were completed at days 1-3-, 25-33, and 60–63-day old flies corresponding to young, middle, and older-aged adults in the fly's lifespan. For each behavioral

assay 50 flies of each sex and genotype were collected and aged in 3 ml fly media vials to account for age related loss.

Behavioral Assays

Y-Maze

Working memory changes between genotypes were closely examined using a y-maze assay (Lewis et al., 2017). Experiments were performed during *Drosophila* peak activity hours 9-10AM and 2-4PM standardized in previous studies from the lab. Two-dimensional movement of individual *Drosophila* was tracked by the Noldus Ethovision software in a y-maze unit comprising 49 individual y-mazes. Assays were conducted in a dark room with each maze uniformly lit from a white LED light box below and flies were covered with a plexiglass coverslip. Flies were given 10 minutes to acclimate to the maze with the lights off. Next, they were given 2 minutes to acclimate to the maze with lights on before the camera (Basler a cA 1300-60gc) collected movement and location data over a 10-minute trial. Movement and location data were summarized by Noldus Ethovision software for individual flies in each trial. Spontaneous alternation behavior was measured by scoring three consecutive arm entries during each 10-minute trial. Y-maze experiments were conducted and pooled between 4 replicates of early (1-3 days old), middle (30-33 days old), and late (60-63 day old) aged flies.

After movement and location data was summarized by Noldus Ethovision software all age points were compiled into a master spreadsheet to be analyzed in R (v. 4.1.2; R Core Team 2021) using R Studio (v.1.4. 1717). Raw data exported from Ethovision was further analyzed through an R script written by Dr. Keating Godfrey. Total movement and percent alternations were processed through R-studio. Total movement is defined by the total distance the fly moves in each trial. Percent alternation displays the fly's ability to travel along a new path which is defined by summarizing each path the fly takes that includes a novel alternating pattern. Percent alternation, total movement calculations were performed for each genotype and sex. Data was pooled among 3-4 replicates. Statistical analyses were conducted using Kruskal-Wallis in Graphpad Prism (v.9.3.1).

Sleep activity

Sleep activity across the fly's lifespan was monitored in individual autoclavable glass tubes (5 mm in diameter and 95 mm in length) with the same fly media that they were aged in. Individual tubes were prepared by melting fly food in the microwave in one-minute intervals and dispensed into the plastic vial end caps until each glass tube had taken up food for ~1-2.5 cm along its length. Food then was cooled to room temperature before flies were loaded for sleep activity monitoring. Flies were placed into individual tubes the day before they reached their appropriate age points. The incubators where the flies were monitored was set to 12-hour light-dark cycle from 9AM-9PM with 25-50% humidity at 25°C. Sleep activity monitoring began at 12AM after placement of flies into the sleep incubator prior to a 6-hour acclimation period. Sleep activity data were collected at one-minute intervals for three days using the *Drosophila Activity Monitoring (DAM)* system (Trikinetics, Waltham, MA) and analyzed using ShinyR-DAM software developed by Hirsh (Cichewicz and Hirsh, 2018).

Using ShinyR (Hirsh, 2018), we measured sleep bout number and duration base on the definition of sleep as 5 minutes of inactivity. Data was pooled from 4 replicates and sleep parameters were analyzed for each genotype across age. Statistical analyses were performed using Kruskal-Wallis once raw data was analyzed using an R-script developed by Dr. Keating Godfrey (unpublished).

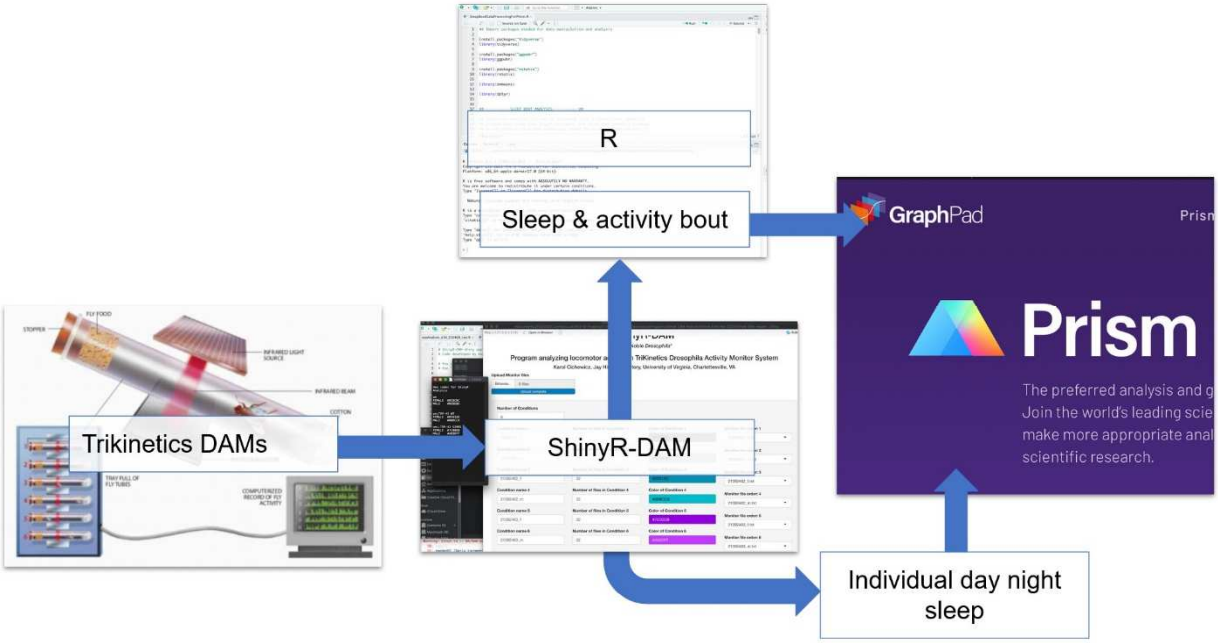

Figure 4. Sleep activity data is collected from Trikinetics DAM system over 3-days. Then uploaded into ShinyR-DAM to be analyzed in R-Studio. Lastly, sleep bout length and number figures are generated in GraphPad Prism. Adapted from Dr. Keating Godfrey.

Mushroom Body Morphology

Mushroom body morphology studies were conducted in female flies across their lifespan for the genotypes listed in Table 1. Non-virgin flies were collected for histology as previous studies in the lab found that anatomy of the mushroom bodies does not alter significantly in virgin versus non-virgin flies. Flies were anesthetized with CO_2 and brains were dissected using forceps in cold physiological HL-3 saline. Next, brains were fixed in 4% paraformaldehyde for 60 minutes at room temperature and subsequently rinsed 3 times in phosphate buffered saline (PBS), permeabilized in a 0.1% Triton X-100 in PBS (PBS-T) for 20 minutes and lastly blocked in 5% normal goat serum with 2% bovine serum albumin in 0.1% PBS-T for 45 minutes before antibody incubation with a concentration of 1:40 mouse anti-Fasciclin-II at room temperature on a rocker overnight. Then washed with 0.1% PBS-T for 3 15-minute rinses. Next, brains were incubated over night at room temperature with secondary antibodies (goat anti-mouse AlexaFluor 568 at a concentration of 1:500 in 0.1% PBS-T. Lastly, brains were incubated for 10 minutes with Hoechst (1:10,000) then mounted in 80% glycerol with propyl gallate on a lysine coated slide for imaging.

Solution	
HL-3 Saline	70 mM NaCL, 5 mM KCL, 22 mM $MgCl_2$, 10 mM $NaHCO_3$, 5 mM trehalose, 15 mM sucrose, 5 mM HEPES at pH 7.3
1X PBS	For 1000 mL, add 78 mL 10X PBS Solution A and 22 mL 10X PBS Solution B and bring to a volume of 1000 mL with ddH_2O and pH to 7.2
10X PBS Solution A	For 500mL, 100mM Na_2HPO_4, 1.3 M NaCL, and pH to 7.2

10X PBS Solution B	For 200 mL, 100mM NaH_2PO_4 H_2O and 1.3 M NaCL and pH to 7.2
1X PBST	For 1000mL, 1 mL Triton X-100 to 1000 mL of 1X PBS for a final concentration of 0.1%
Block	PBST with 2% BSA and 5% Normal Goat serum, filter sterilized. For every 100 mL PBS, 0.1 mL Triton X-100, 2 g Bovine Serum Albumin, 5 mL Normal Goat serum.

Table 2. Buffers and reagents used for immunofluorescence studies of MB morphology

Reagent	Source	Identifier
Primary Antibody: mouse anti-Fasciclin-II (ID4) 1:40	DSHB	RRID: AB_528235
Secondary Antibody: Polyclonal Alexa Fluor-568-conjugated goat anti-mouse 1:500	ThermoFisher Scientific	Cat#A-11004;RRID: AB_2534072
Hoechst Trihydrochloride, Trihydrate 1:10000	ThermoFisher Scientific	H3570
4% Paraformaldehyde in PBS	Santa Cruz Biotechnology	sc-281692

Table 3. Commercially available reagents and antibodies used for immunofluorescence studies of MB morphology.

All images were acquired using a Zeiss LSM 880 inverted confocal microscope with a Plan-Apochromat 40x oil DIC m27 lens. The pinhole was adjusted to 1 AU and 40 µm optical section thickness. Z-stacks were processed, and mushroom body marker anti-Fasciclin-II was used to label MBs. Geometric measurements (width and length) of each mushroom body lobe (α,β,γ) were taken between age and genotype using Fiji ImageJ (v.153). GraphPad was used to perform two-way ANOVA tests were utilized to compare mushroom body lobe thinning between genotypes and age variables.

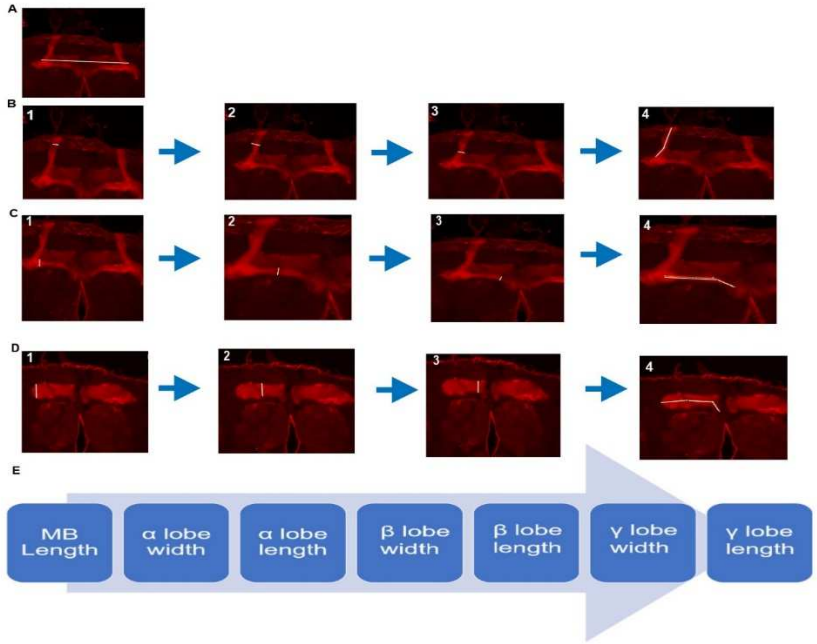

Figure 5. MB geometric measurement

Geometric measurements of the MB lobes were taken to measure lobe thinning. Panel A shows the first measurement taken of the full length of the MB to standardize all subsequent lobe length measurements. Panel B: 1-3 illustrate the alpha lobe width measurements taken starting with the top of the α lobe to where the γ lobe is visible. Panel B:4 is the total length of the α lobe. Panels C: 1-3 demonstrate the β lobe width measurements taken. Panel C:4 shows the total length of the β lobe collected. Panel D 1-3 show the γ lobe width measurements taken and lastly in Panel D:4 the total length of the γ lobe collected. Panel E shows the workflow of how the MB geometric measurements are taken.

Results

Our first aim of this study was to identify FTD symptom contribution between HRE RNA versus DPR polyGR toxicity. To distinguish the two, we used the mushroom body specific spGAL4 SS01276 to express RNA-only G4C2 repeats or ATG driven dipeptide GR repeats under the control of the UAS promoter. Previous studies identified arginine containing GR and PR DPRs as the predominant toxic protein species in this model, although all five DPR proteins

form inclusions in affected brain regions (Isaacs, 2014). See Methods for more information on the specific genetic constructs used in this study.

Modeling FTD disease pathology in Drosophila can provide valuable insights into the cellular-level mechanisms within an intact organism. The aim of this study is to probe for the presence of FTD relevant phenotypes using behavioral assays such as Y-maze (working memory) and sleep, two behaviors found to be altered in patients (Nicholas-Tiberio Economou, 2014). Clinical diagnoses of "possible" behavior variant FTD requires three of a possible six discriminating features (disinhibition, apathy/inertia, loss of sympathy/empathy, perseverative/compulsive, hyperorality and dysexecutive neurophysiological behaviors) as defined in (Rascovsky et al., 2011a). Additionally, recent studies have shown that the behavior variant of FTD has exhibited episodic memory deficits by performing comparably to Alzheimer's Disease (AD) patients on verbal and visual recognition and recall tests (Pennington et al., 2011). To examine the robustness of our Drosophila c9orf72 expression model we employed a Y-Maze assay to evaluate the fly's ability to develop spatial working memory (Lewis *et al.*, 2017). In addition, sleep activity monitoring to evaluate any indications of abnormal sleep fragmentation was performed. A second aim of the study is to closely examine MB lobe thinning as C9orf72 patients with the hexanucleotide repeat expansion (HRE) display brain atrophy. In particular (G4C2) hexanucleotide repeats have been found in the frontal cortex in FTD patient brain tissues (Renton *et al.*, 2011). Another research study uncovered that the number of C9orf72 hexanucleotide correlated with the severity of FTD disease symptoms (Shaw and Kirby, 2014). The MB region of the Drosophila brain is responsible for many behavioral FTD phenotypes including olfactory learning and memory, decision making, sleep regulation, appetite, and social behavior (Pitman et al., 2006); (Turner et al., 2008); (Zhu, 2020); (Chen-Han and Lin, 2018). Previous studies in Drosophila models of Alzheimer's disease showed that overexpression of Tau protein induced neurodegeneration as indicated by immunostaining for Fasciclin-II, a marker for MB neurons (Gistelinck et al., 2012). Our study used Anti-Fasciclin-II antibodies to better understand morphological changes in mushroom body anatomy in a Drosophila model of C9orf72 expression.

Behavioral assay results

Working memory/Movement

To evaluate working memory, we utilized a well-established Y-maze assay, recently adapted to use in *Drosophila*. In this assay, individual flies are placed in miniature Y mazes and evaluated for their ability to alternate between the three arms within a 12-minute period (see Methods and Figure 6). When analyzing alternation, we noticed genotype and age dependent changes in total movement which we included in our analyses. We found that males overexpressing RNA only HREs (w^{1118}; UAS (G4C2) 108X RO attP40) displayed hyperactivity as indicated by an increase in movement at both young and old age points, compared to controls (w^{1118}; UAS (G4C2) 3X attP40) (Figures 7-9). Additionally, females expressing RNA only HREs (w^{1118}; UAS (G4C2) 108X RO attP40) exhibited an increase in movement at the middle

age timepoint compared to controls. Lastly, females expressing polyGR repeats (w^{1118}; UAS PolyGR 100X attP40) showed a significant increase in movement at young and old age timepoints compared to genetic background controls (w^{1118}; attP40). When we normalized percent alternation to the fly's total distance moved no differences were observed (Figures 12-14). Therefore, this assay shows that although the flies may show changes in alternation, the impact of C9orf72 on working memory is confounded by changes in movement, in an age and genotype dependent manner. Future studies can use the data collected through Ethovision to explore alternative phenotypes that these C9orf72 hexanucleotide repeat expansions or DPRs could be causing.

To determine memory and movement changes caused by either G4C2 HREs or polyGR DPRs compared to their respective controls we examined individual genotypes in an age dependent manner (Figures 10-11). These experiments showed that male polyGR repeats (w^{1118}; UAS PolyGR 100X attP40) displayed a significant in distance moved from their young to their middle age time point Figure 10 B). Comparing across genotypes young and old RNA only HREs (w^{1118}; UAS (G4C2) 108X RO attP40) males demonstrated a significant increase in distance moved compared to their genetic control (w^{1118}; UAS (G4C2) 3X attP40) (Figure 10 C). Overall, there were no significant changes in percent alternation. All results are summarized in Tables 4 and 5.

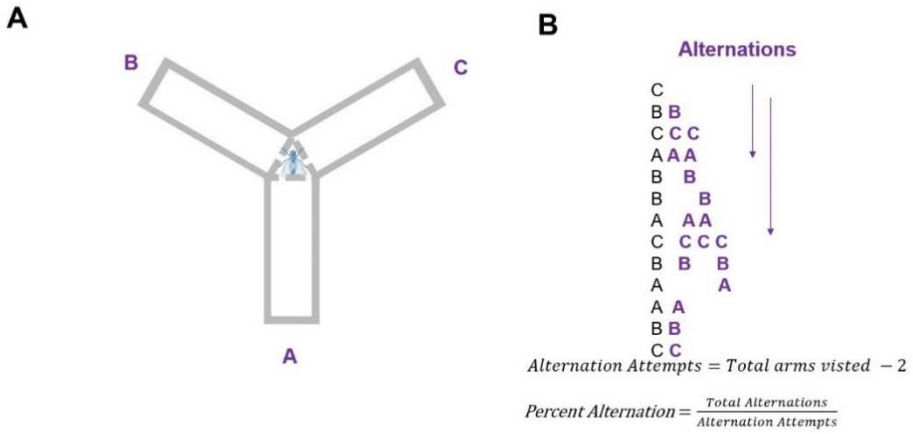

Figure 6. (A) Representation of spatial working memory assay showing the sequence of decisions made (B) by a fly (black text) and their corresponding alternations (purple). Percent alternation is calculated as total alternations divided by alternation attempts. Adapted figure from Dr. Keating Godfrey.

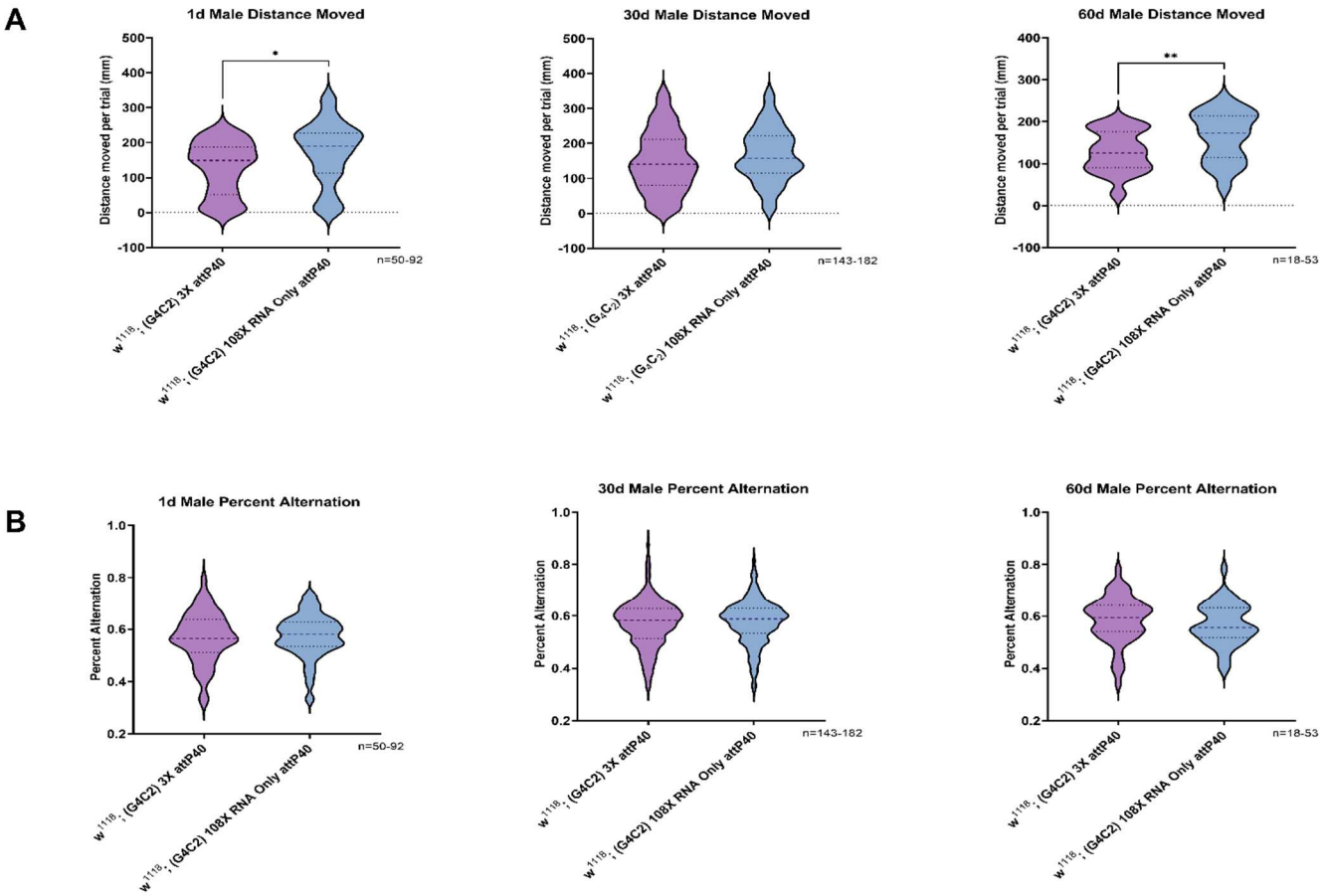

Figure 7. (A) Comparison between RNA only HREs (w^{1118}; UAS (G4C2) 108X RO attP40) and w^{1118}; UAS (G4C2) 3X attP40 genetic background control shows that young (1-3 day) old flies and old (60-63 day) flies show significant decreases in movement. (B) Flies show no significant changes in percent alternation. * = $p < 0.01$, ** = $p < 0.006$

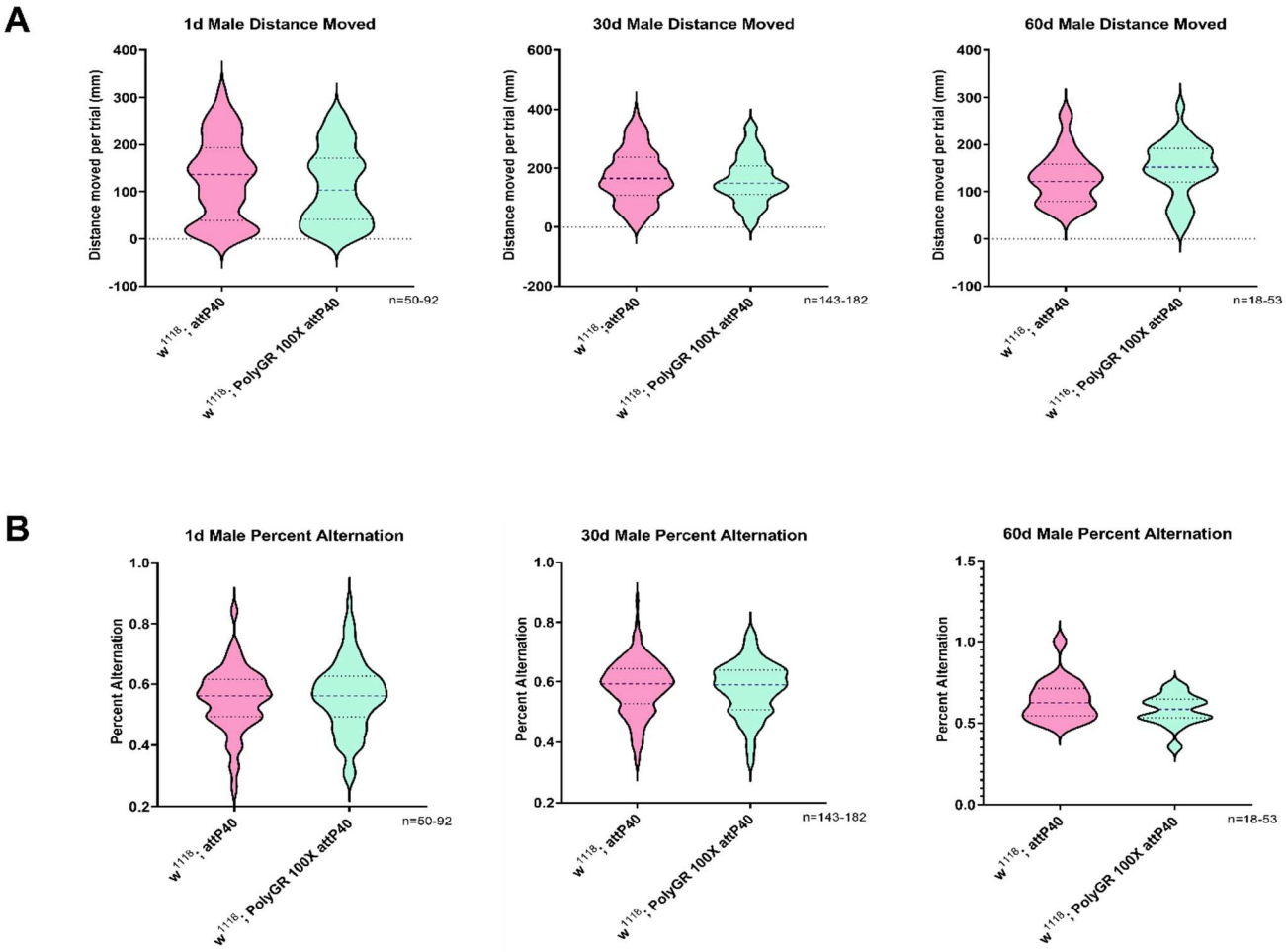

Figure 8. No significant changes among polyGR repeat *(*w^{1118}; UAS PolyGR 100X attP40) compared to genetic background control w^{1118}; attP40.

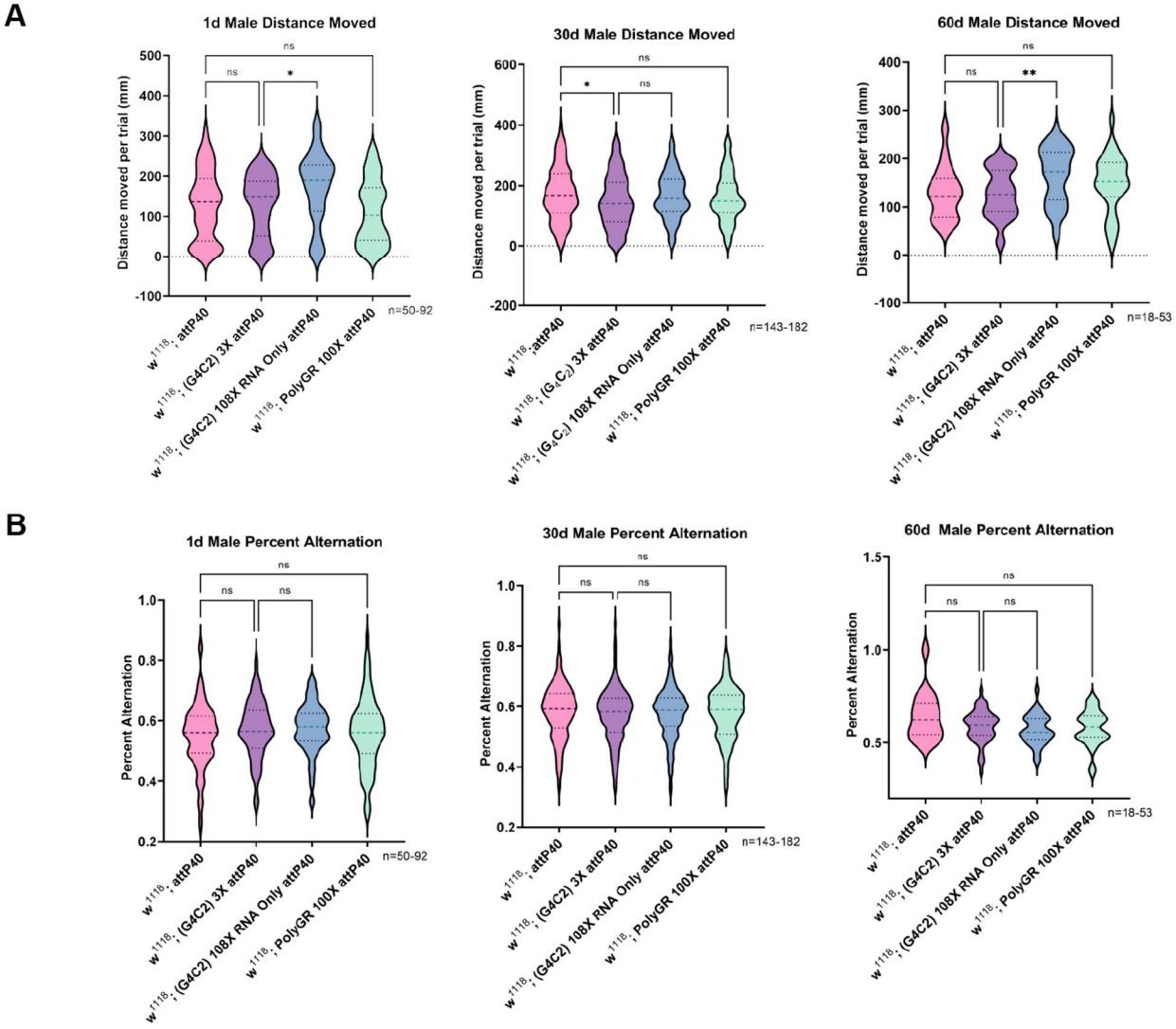

Figure 9. (A) Young (1-3 day) old flies and old (60-63 day) RNA only HREs (w^{1118}; UAS (G4C2) 108X RO attP40) flies show significant increases in movement. (B) Flies show no significant changes in percent alternation. * = p <0.01 , ** = p <0.001

Table 4. Summary of male working memory results showing an increase in distance moved by RNA only HREs (w1118 ; UAS (G4C2) 108X RO attP40) at young and old age points compared to genetic background control (w1118; UAS (G4C2) 3X attP40)

Genotype	**Age(days)**	**Phenotype**
w^{1118}; attP40	3	None
w^{1118}; attP40	30	None
w^{1118}; attP40	60	None
w^{1118}; UAS (G4C2) 3X attP40	3	Distance moved: Decrease Percent alternation: No change
w^{1118}; UAS (G4C2) 3X attP40	30	None

w^{1118}; UAS (G4C2) 3X attP40	60	Distance moved: Decrease Percent alternation: No change
w^{1118}; UAS (G4C2) 108X RO attP40	3	Distanced moved: Increase Percent alternation: No change
w^{1118}; UAS (G4C2) 108X RO attP40	30	None
w^{1118}; UAS (G4C2) 108X RO attP40	60	Distanced moved: Increase Percent alternation: No change
w^{1118}; UAS PolyGR 100X attP40	3	None
w^{1118}; UAS PolyGR 100X attP40	30	None

w^{1118}; UAS PolyGR 100X attP40	60	None

Male results across lifespan

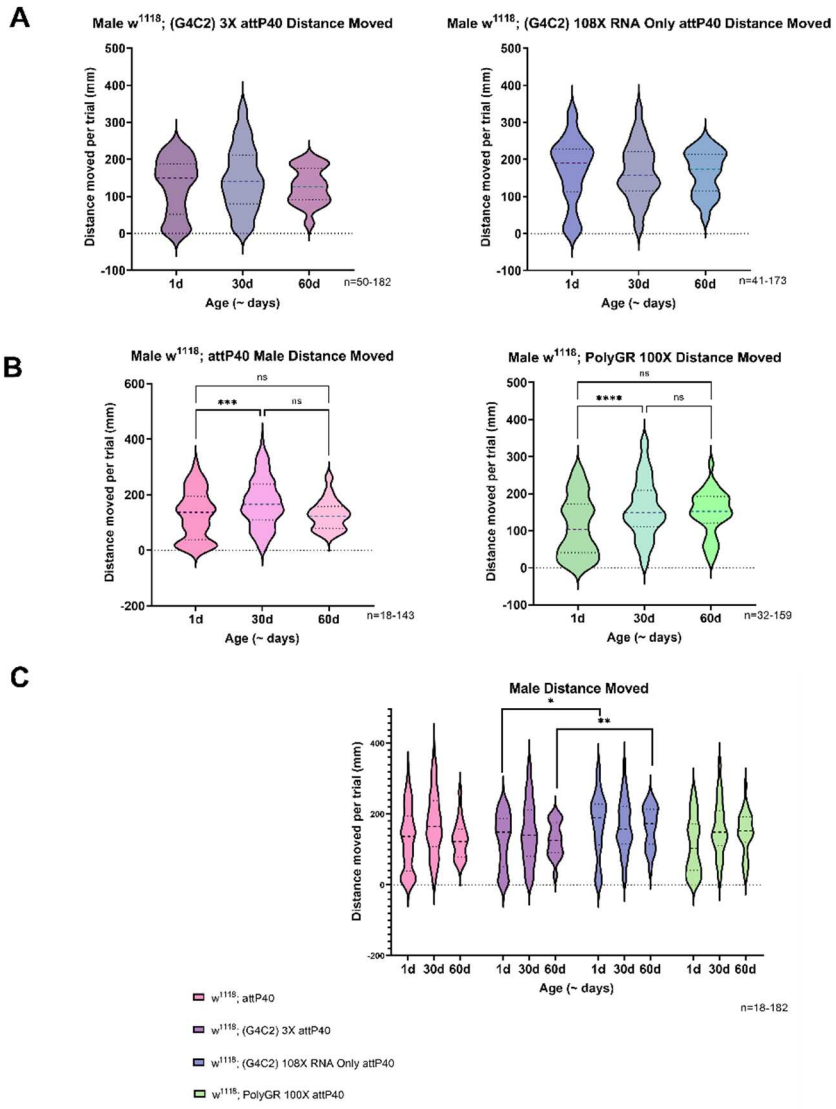

Figure 10. Male genetic background control (w^{1118}; attP40) have an increase in distance moved from young and middle age time point (B). Male polyGR repeat (w^{1118}; UAS PolyGR 100X attP40*)* have an increase in distance moved from young to the middle age time point. 1-3d and 60d male RNA only HREs (w^{1118}; UAS (G4C2) 108X RO attP40) have an increase in distance

moved to their (w^{1118}; UAS (G4C2) 3X attP40) genetic background control. Additionally, male w^{1118}; attP40 genetic background control young flies showed a significant increase from their middle and old age points (C).

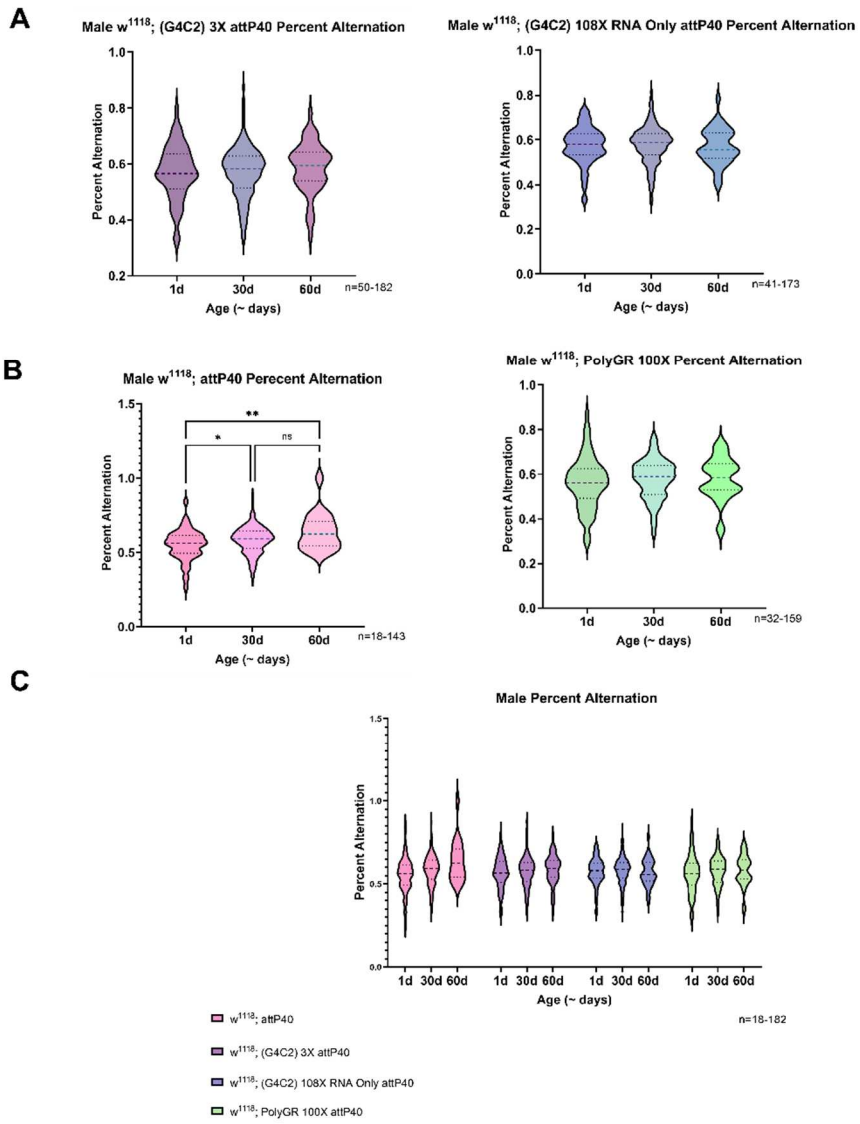

Figure 11. Male w^{1118}; attP40 genetic background control young flies showed an age dependent increase in alternation during lifespan Panel (B).

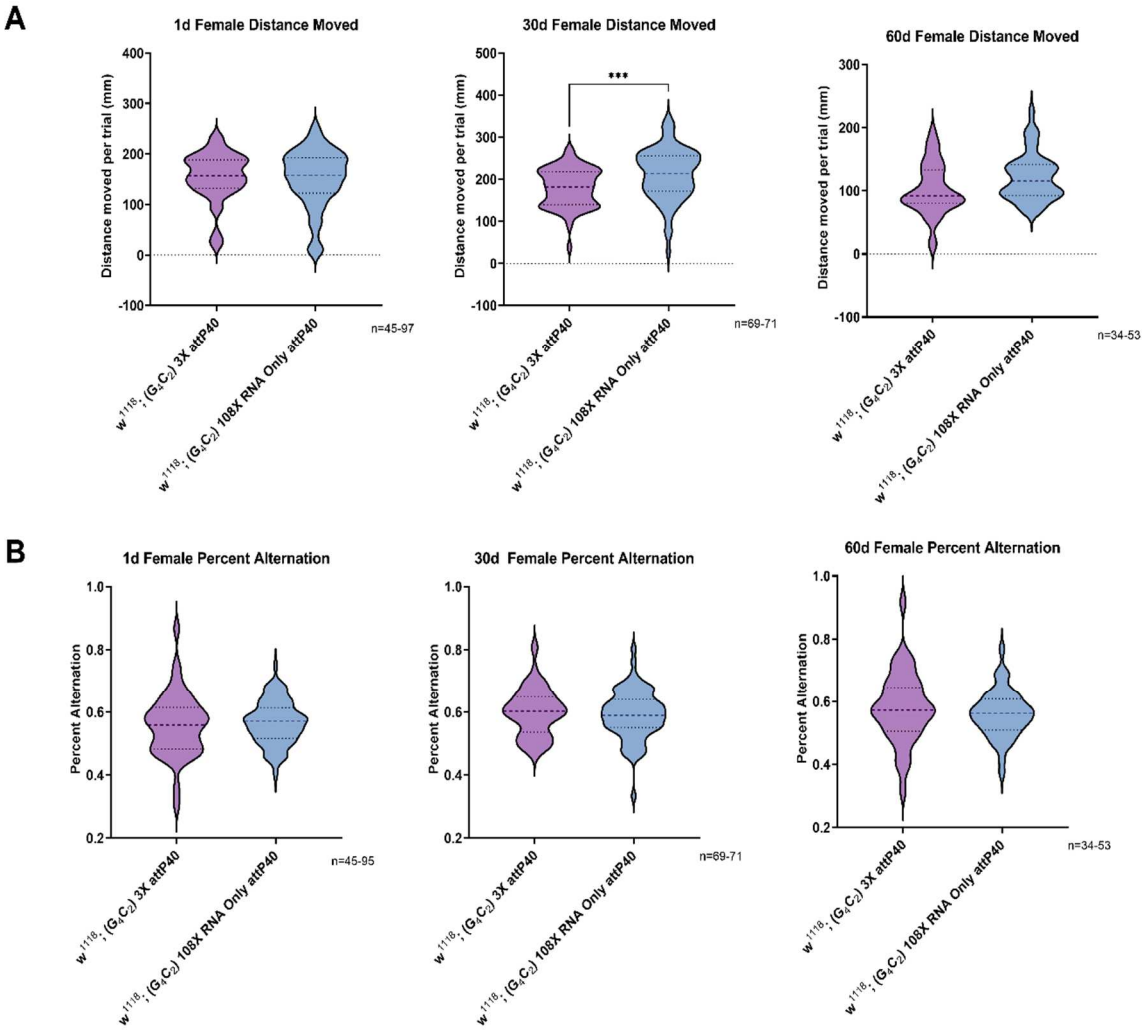

Figure 12. Female middle-aged RNA only HREs (w^{1118}; UAS (G4C2) 108X RO attP40) flies show significant increases in movement (A). *** = p <0.0006 , **** = p <0.0001

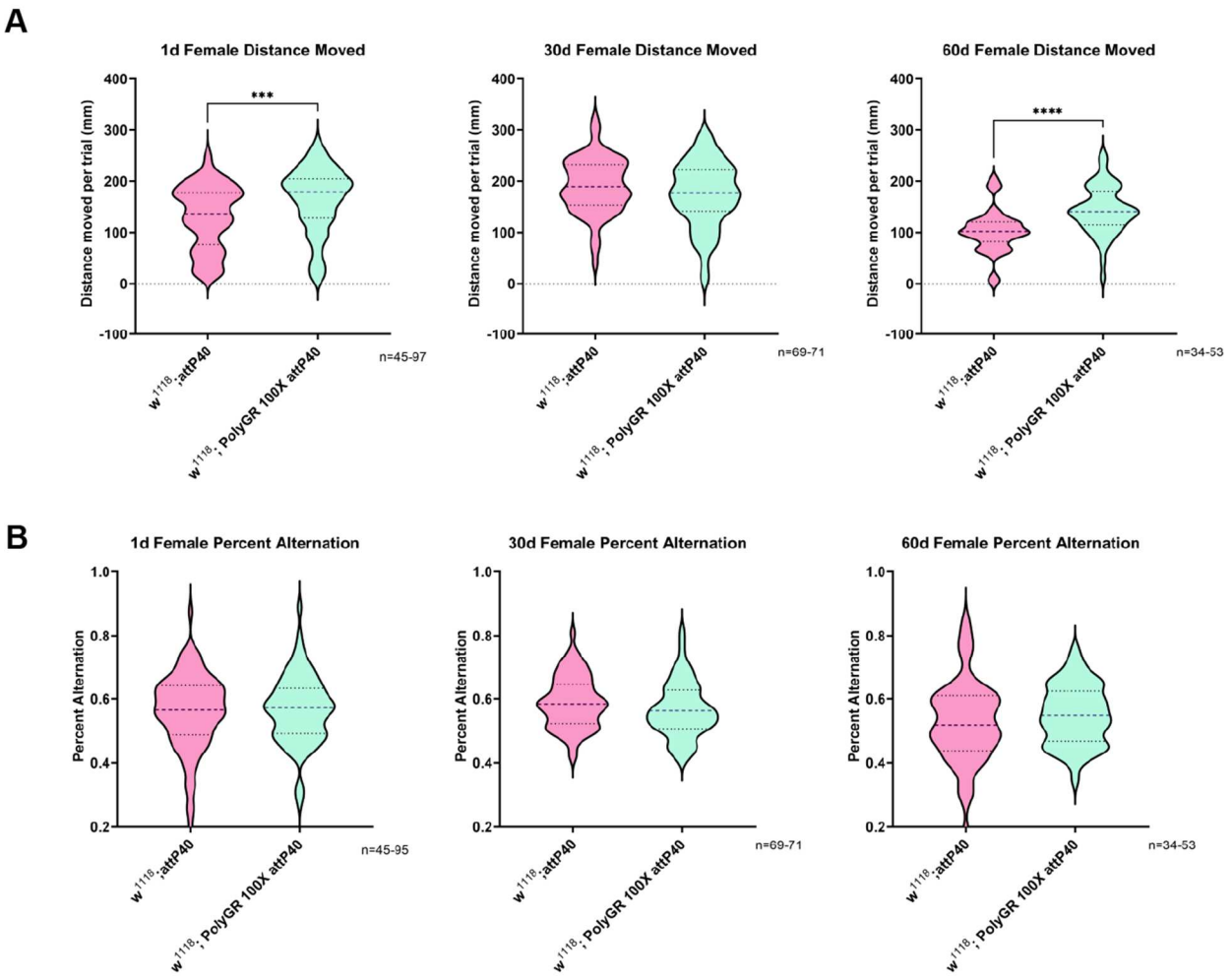

Figure 13. (A) Young female (1-3 day) old flies and old (60-63 day) polyGR repeat (w^{1118}; UAS PolyGR 100X attP40) have a significant increase in movement. *** = p <0.0006 , **** = p <0.0001

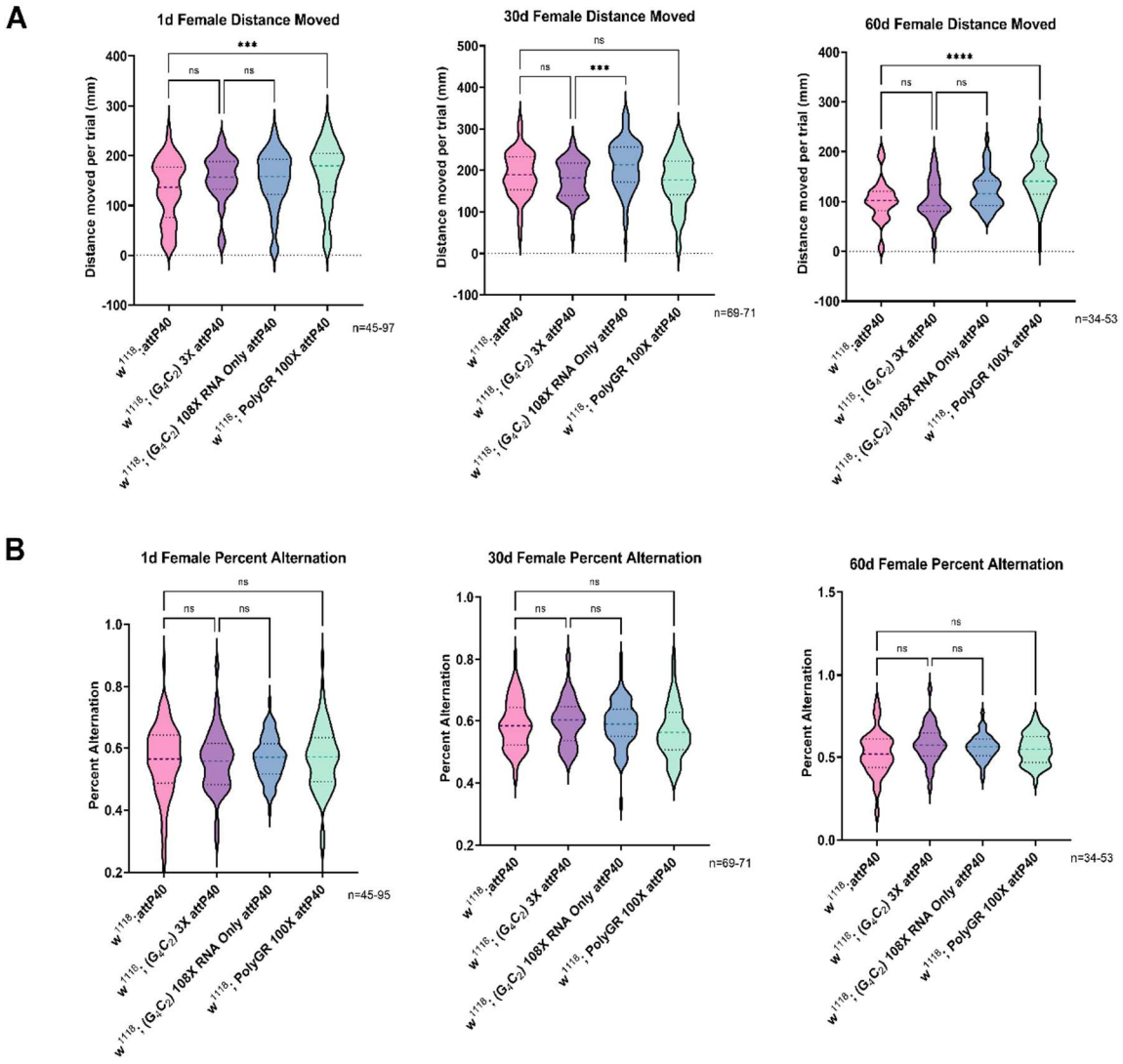

Figure 14. (A) Young female (1-3 day) old flies and old (60-63 day) polyGR repeat (w^{1118}; UAS PolyGR 100X attP40) have a significant increase in movement. Female middle-aged RNA only HREs (w^{1118}; UAS (G4C2) 108X RO attP40) flies show significant increases in movement. (B). *** = p <0.0006 , **** = p <0.0001

Table 5. Summary of female working memory results showing an increase in distance moved by polyGR repeat (w^{1118}; UAS PolyGR 100X attP40) at young and old age points compared to its comparable control (w^{1118}; attP40). And an increase in distance moved by RNA only HREs (w^{1118}; UAS (G4C2) 108X RO attP40) in middle age.

Genotype	Age (days)	Phenotype
w^{1118}; attP40	3	None
w^{1118}; attP40	30	None
w^{1118}; attP40	60	None
w^{1118}; UAS (G4C2) 3X attP40	3	None
w^{1118}; UAS (G4C2) 3X attP40	30	Distance moved: Decrease

		Percent alternation: No change
w^{1118}; UAS (G4C2) 3X attP40	60	None
w^{1118}; UAS (G4C2) 108X RO attP40	3	None
w^{1118}; UAS (G4C2) 108X RO attP40	30	Distance moved: Increase Percent alternation: No change
w^{1118}; UAS (G4C2) 108X RO attP40	60	None
w^{1118}; UAS PolyGR 100X attP40	3	Distance moved: Increase Percent alternation: No change

w^{1118}; UAS PolyGR 100X attP40	30	None
w^{1118}; UAS PolyGR 100X attP40	60	Distance moved: Increase Percent alternation: No change

Female results across lifespan

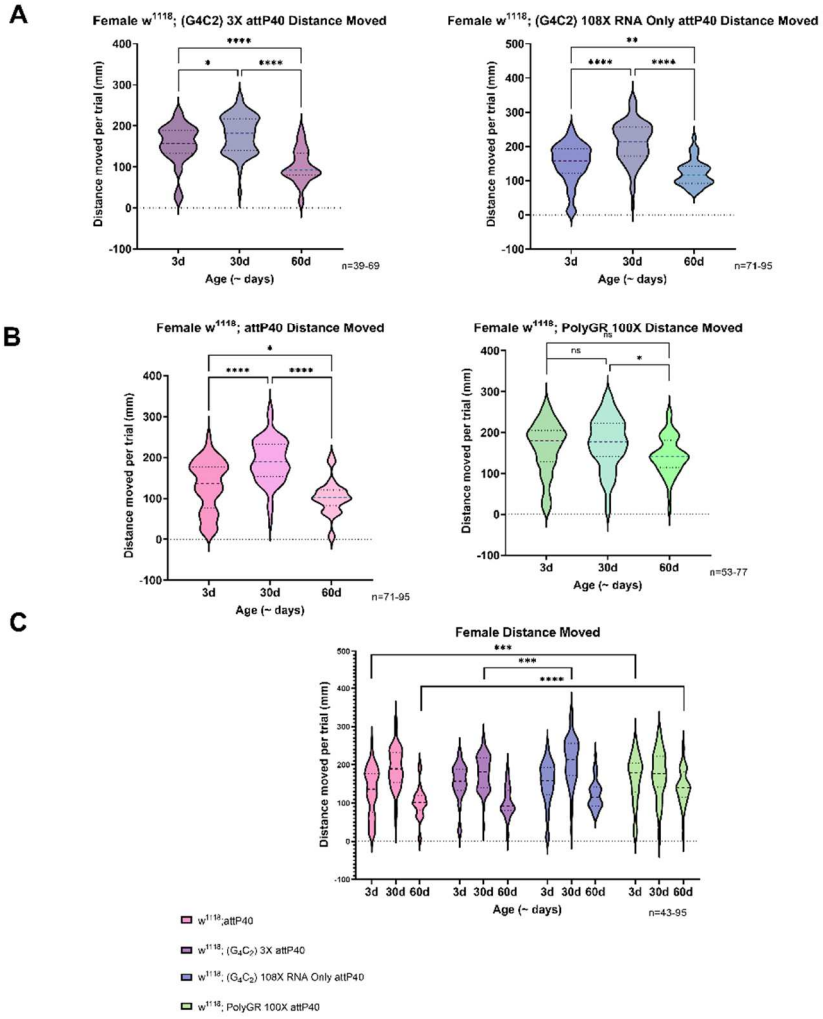

Figure 15. Female young age flies have a significant increase in distance moved (w^{1118}; UAS (G4C2) 3X attP40) while old, aged flies have a significant decrease in distance moved (A). Young and old w^{1118}; attP40 flies have a decrease in distance moved compared to polyGR repeat (w^{1118}; UAS PolyGR 100X attP40) (C).

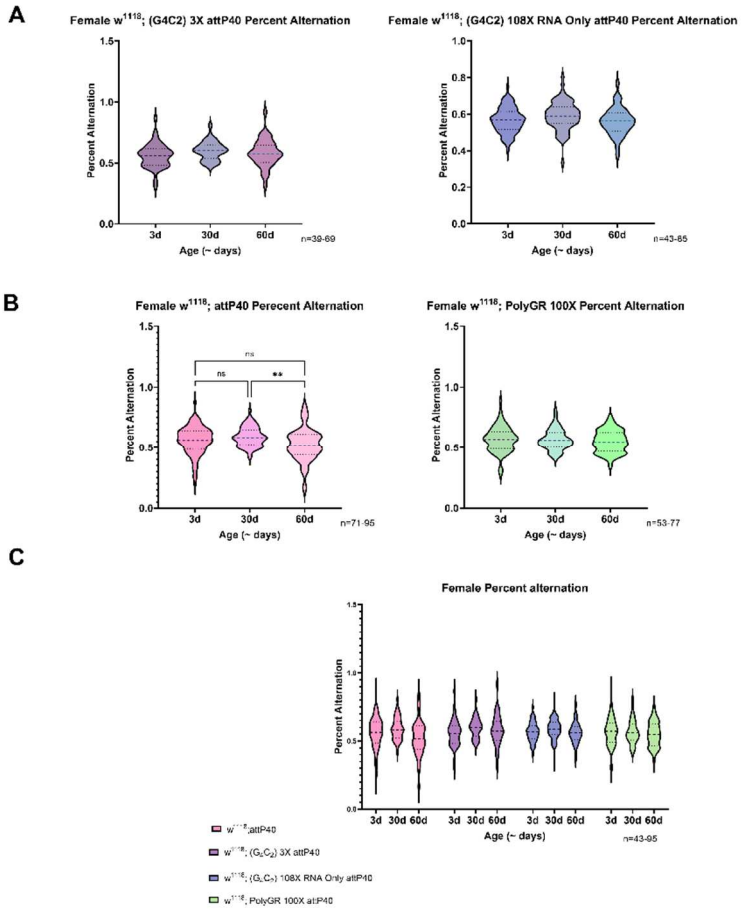

Figure 16. Middle aged female w^{1118}; attP40 flies have a significant reduction in percent alternation compared to old age (B).

Sleep Activity

The MB region of the Drosophila brain is responsible for many behavioral FTD relevant phenotypes including olfactory learning and memory, decision making, sleep regulation, appetite, and social behavior Pitman *et al.* (2006);Turner *et al.* (2008);Zhu (2020);Chen-Han and Lin (2018). To evaluate sleep abnormalities, we monitored activity, with *Drosophila* sleep activity being defined as 5 minutes of inactivity Shaw et al. (2000). FTD is associated with an increased daytime drowsiness, but overall sleep disturbances have been highly variable in human cases of FTD and may be detectable in earlier stages compared to AD (Economou et al., 2014). This study employed young, middle, and old flies that expressed C9orf72 in the MB neurons.

Our sleep assays showed that male RNA only HREs (w^{1118}; UAS (G4C2) 108X RO attP40) flies at a young age show an increase in sleep bout number and length. Older flies exhibit elevated sleep bout numbers; however, no change was detected in sleep bout length (Figure 18). Additionally, polyGR repeat (w^{1118}; UAS PolyGR 100X attP40) flies exhibit a reduction in day sleep bout number at middle and old age points (Figure 19). Whereas young RNA only HREs (w^{1118}; UAS (G4C2) 108X RO attP40) female flies exhibit a decrease in arousal and an increase in sleep arousal in middle age (Figure 26). Furthermore, polyGR repeat (w^{1118}; UAS PolyGR 100X attP40) flies show sleep fragmentation at a young age, with an overall increase in night sleep bout length in old age (Figure 27). All results are summarized in Table 6-7 and 8-9.

Additionally, we examined any sleep activity differences across the fly's lifespan and found that in addition to genotype differences from C9orf72 hexanucleotide repeats versus dipeptide repeats there appears to be sex differences. This is shown by male 60-day RNA only HREs (w^{1118}; UAS (G4C2) 108X RO attP40) flies having higher sleep bout lengths and numbers. With 60-day polyGR repeat (w^{1118}; UAS PolyGR 100X attP40) flies having a reduction in day and sleep bout length with greater number of night sleep bouts (Figures 22-25). Additionally, young RNA only HREs (w^{1118}; UAS (G4C2) 108X RO attP40) females exhibited an increase sleep bout number and length. Lastly, polyGR repeat (w^{1118}; UAS PolyGR 100X attP40) flies had a reduction in day and night sleep bout length (Figures 29-33).

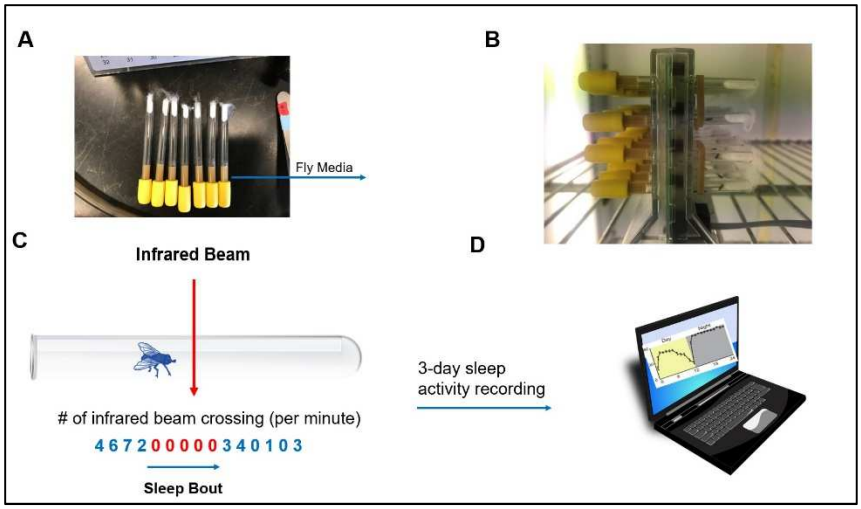

Figure 17. Sleep activity was monitored across the fly's lifespan by carefully placing individual flies into autoclavable sleep chambers with the same fly media that they were aged in (A). 32 flies of each genotype and sex were loaded into the Drosophila Activity Monitoring system (B) (Trikinetics, Waltham, MA). Flies were placed in an incubator on a 12-hour light-dark cycle for a period of 3 days. Sleep activity data was collected at 1-minute intervals where an infrared beam break was deemed as the fly being active (C). A sleep bout is defined as a fly having no beam breaks over a 5-minute interval. Sleep activity was recorded using the Drosophila Activity Monitoring system (D).

1A

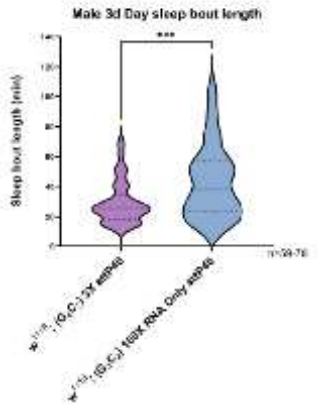

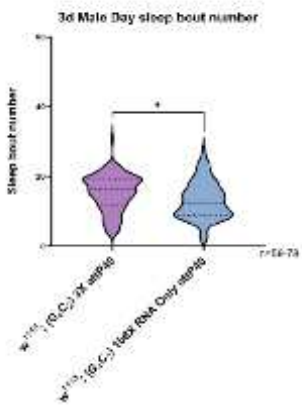

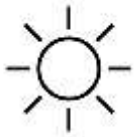

Day Sleep bout length (Right)

Day Sleep bout number (Left)

1B

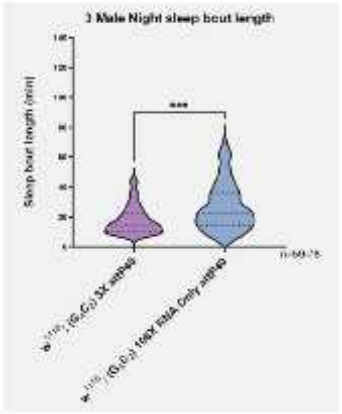

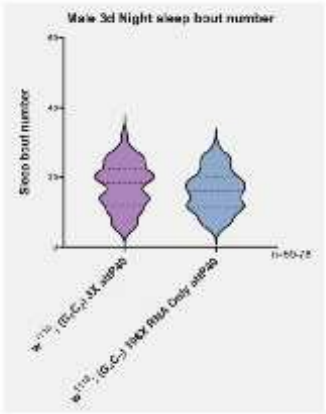

Night Sleep bout length (Right)

Night Sleep bout number (Left)

2A

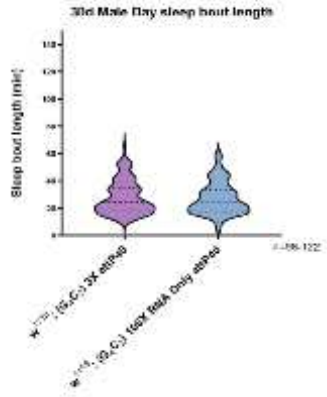

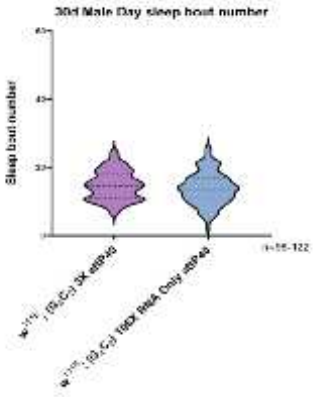

2B

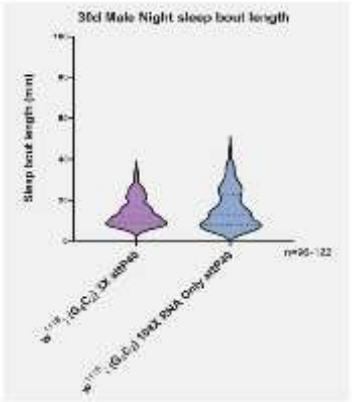

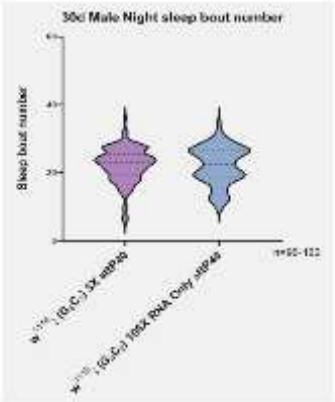

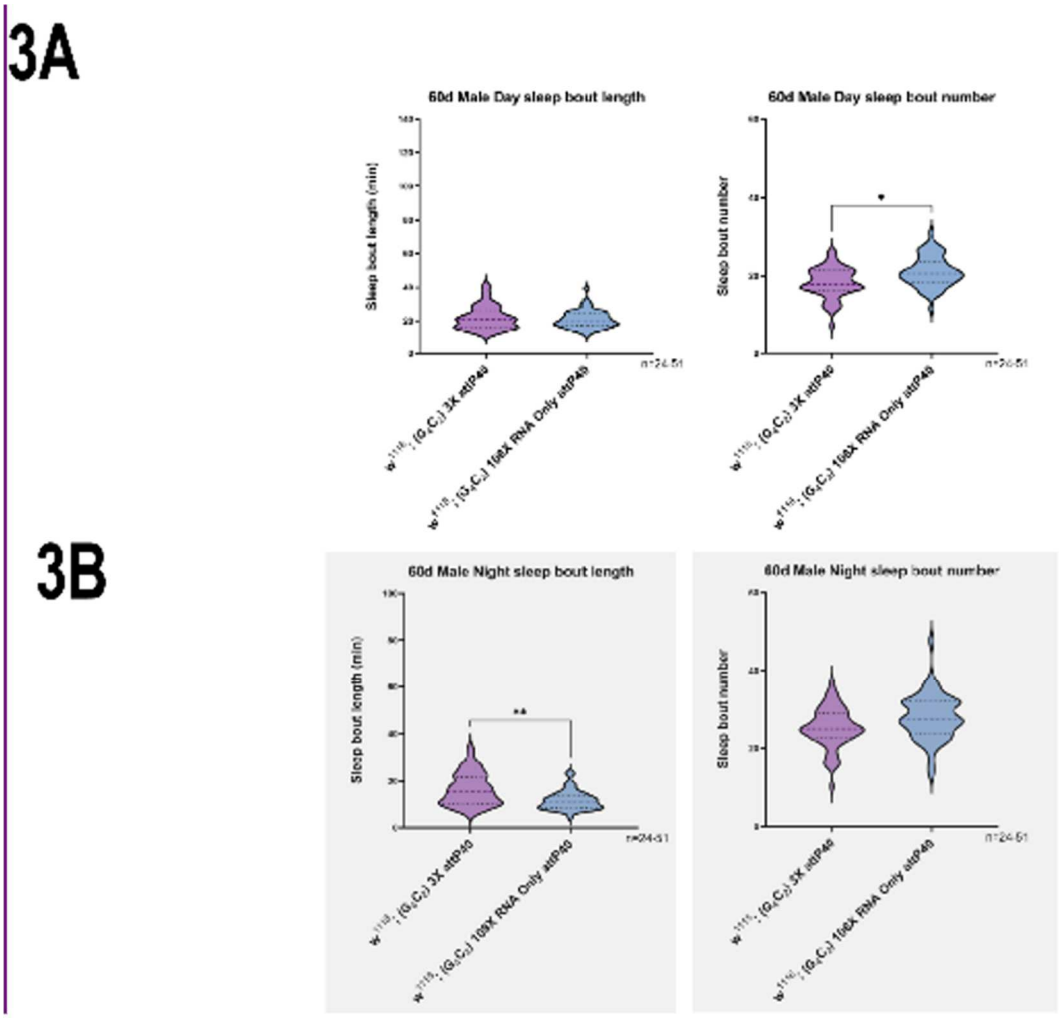

Figure 18. RNA only HREs (w^{1118}; UAS (G4C2) 108X RO attP40) flies have an increased day sleep bout length and a reduction in sleep bout number at 3-days (1A). No significant changes in sleep activity occurs at middle age (2A-2B). At 60-days RNA only HREs (w^{1118}; UAS (G4C2) 108X RO attP40) flies have a slight increase in day sleep bout number and a reduction in sleep bout length compared to (w^{1118}; UAS (G4C2) 3X attP40) genetic background control (3A-3B).

1A

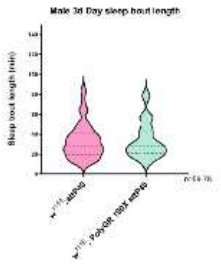

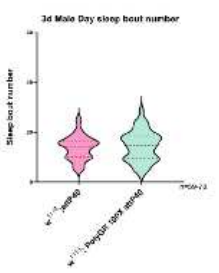

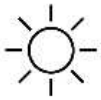

Day Sleep bout length (Right)

Day Sleep bout number (Left)

1B

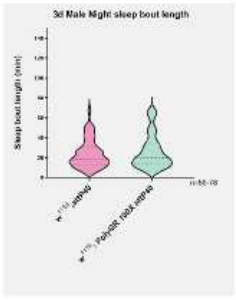

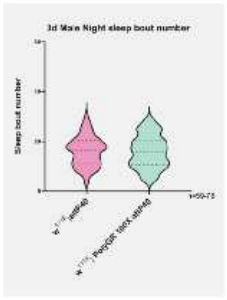

Night Sleep bout length (Right)

Night Sleep bout number (Left)

2A

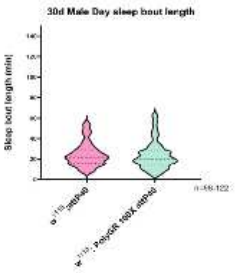

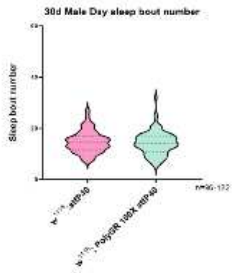

2B

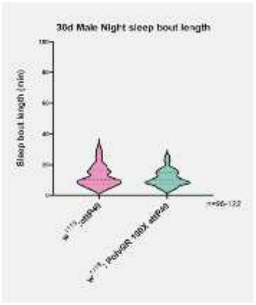

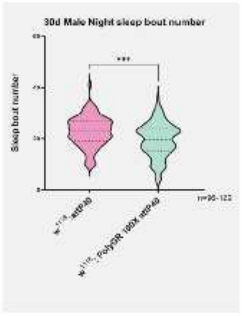

3A

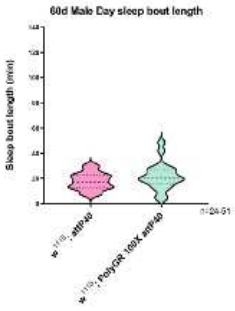

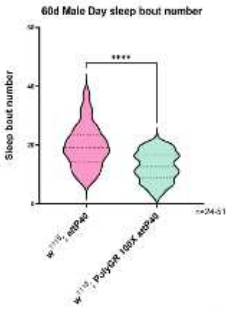

3B

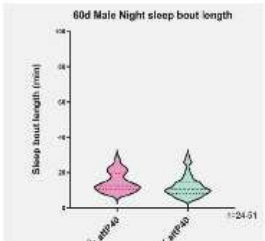

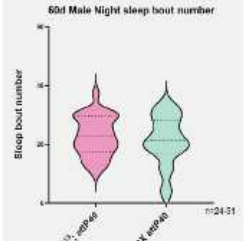

Figure 19. Male polyGR repeat (w^{1118}; UAS PolyGR 100X attP40) flies at a young age show no change in day or night sleep (1A-1B). While middle aged flies have a decrease in sleep bouts and similar sleep bout length (2A-2B). In contrast, older polyGR repeat (w^{1118}; UAS PolyGR 100X attP40) flies have a significant reduction in day sleep bouts while no change in night sleep bout number compared to w^{1118}; attP40 genetic background control (3A-3B).

1A

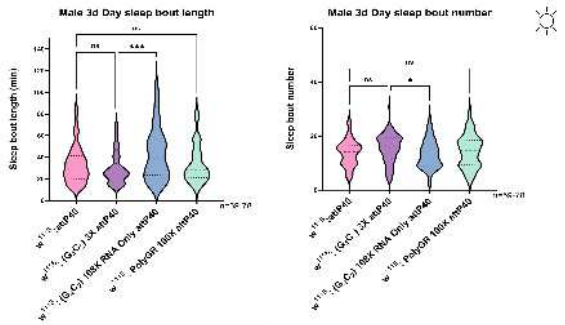

Day Sleep bout length (Right)

Day Sleep bout number (Left)

1B

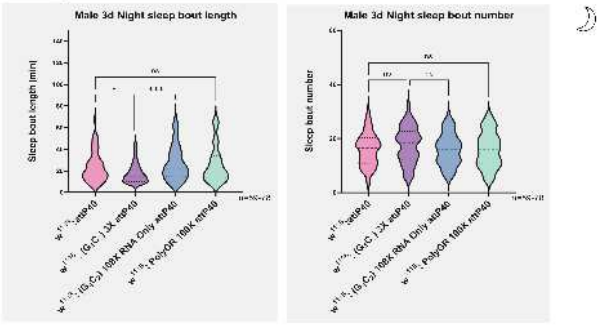

Night Sleep bout length (Right)

Night Sleep bout number (Left)

2A

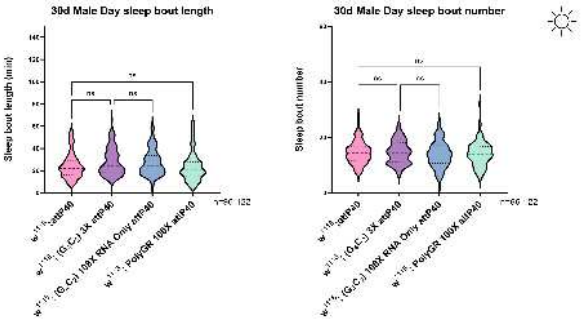

2B

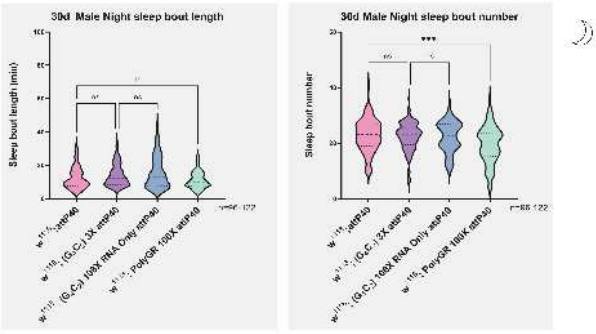

3A

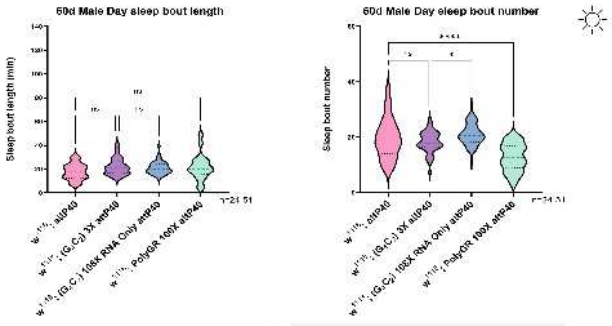

3B

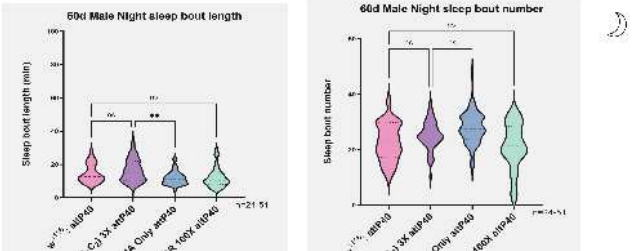

Figure 20. Male RNA only HREs (w^{1118}; UAS (G4C2) 108X RO attP40) flies have an increase in day and night sleep bout length during young age (1A-1B). 30-day polyGR repeats (w^{1118}; UAS PolyGR 100X attP40) flies have a reduction in night sleep bout number (2B). At older age RNA only HREs (w^{1118}; UAS (G4C2) 108X RO attP40) have an increase night sleep length and increase in number of sleep bouts during the day (3A-3B). While polyGR repeats (w^{1118}; UAS PolyGR 100X attP40) flies have a reduction in day sleep bout number at 60-day (3B).

Table 6. Summary of male day sleep results showing an increase in sleep bout number and length at an early age by RNA only HREs (w^{1118}; UAS (G4C2) 108X RO attP40) compared to controls (w^{1118}; UAS (G4C2) 3X attP40). Old RNA only HREs (w^{1118}; UAS (G4C2) 108X RO attP40) flies shows an increase in sleep bout number, but no change in sleep bout length. Additionally, polyGR repeats (w^{1118}; UAS PolyGR 100X attP40) at young age show no change in sleep bout length, but an increase in sleep bout number age points compared to genetic background controls (w^{1118}; attP40).

Genotype	**Age (days)**	**Phenotype**
w^{1118}; attP40	3	None
w^{1118}; attP40	30	None
w^{1118}; attP40	60	None

w^{1118}; UAS (G4C2) 3X attP40	3	Sleep bout length: Decrease Sleep bout number: Decrease
w^{1118}; UAS (G4C2) 3X attP40	30	None
w^{1118}; UAS (G4C2) 3X attP40	60	Sleep bout length: No change Sleep bout number: Decrease
w^{1118}; UAS (G4C2) 108X RO attP40	3	Sleep bout length: Increase Sleep bout number: Increase
w^{1118}; UAS (G4C2) 108X RO attP40	30	None
w^{1118}; UAS (G4C2) 108X RO attP40	60	Sleep bout length: No change Sleep bout number: Increase

w^{1118}; UAS PolyGR 100X attP40	3	None
w^{1118}; UAS PolyGR 100X attP40	30	Sleep bout length: Sleep bout number:
w^{1118}; UAS PolyGR 100X attP40	60	Sleep bout length: No change Sleep bout number: Decrease

Table 7. Male night sleep results show that early age RNA only HREs (w^{1118}; UAS (G4C2) 108X RO attP40) display an increase in sleep bout length, while at an old age they exhibit a decrease compared to (w^{1118}; UAS (G4C2) 3X attP40). Additionally, middle aged polyGR repeats (w^{1118}; UAS PolyGR 100X attP40) flies show a decrease in night sleep bout number.

Genotype	**Age (days)**	**Phenotype**
w^{1118}; attP40	3	None

w^{1118}; attP40	30	None
w^{1118}; attP40	60	None
w^{1118}; UAS (G4C2) 3X attP40	3	Sleep bout length: Decrease Sleep bout number: No change
w^{1118}; UAS (G4C2) 3X attP40	30	None
w^{1118}; UAS (G4C2) 3X attP40	60	Sleep bout length: Increase Sleep bout number: No change
w^{1118}; UAS (G4C2) 108X RO attP40	3	Sleep bout length: Increase Sleep bout number: No change

w^{1118}; UAS (G4C2) 108X RO attP40	30	None
w^{1118}; UAS (G4C2) 108X RO attP40	60	Sleep bout length: Decrease Sleep bout number: None
w^{1118}; UAS PolyGR 100X attP40	3	None
w^{1118}; UAS PolyGR 100X attP40	30	Sleep bout length: No change Sleep bout number: Decrease
w^{1118}; UAS PolyGR 100X attP40	60	None

Male sleep across lifespan

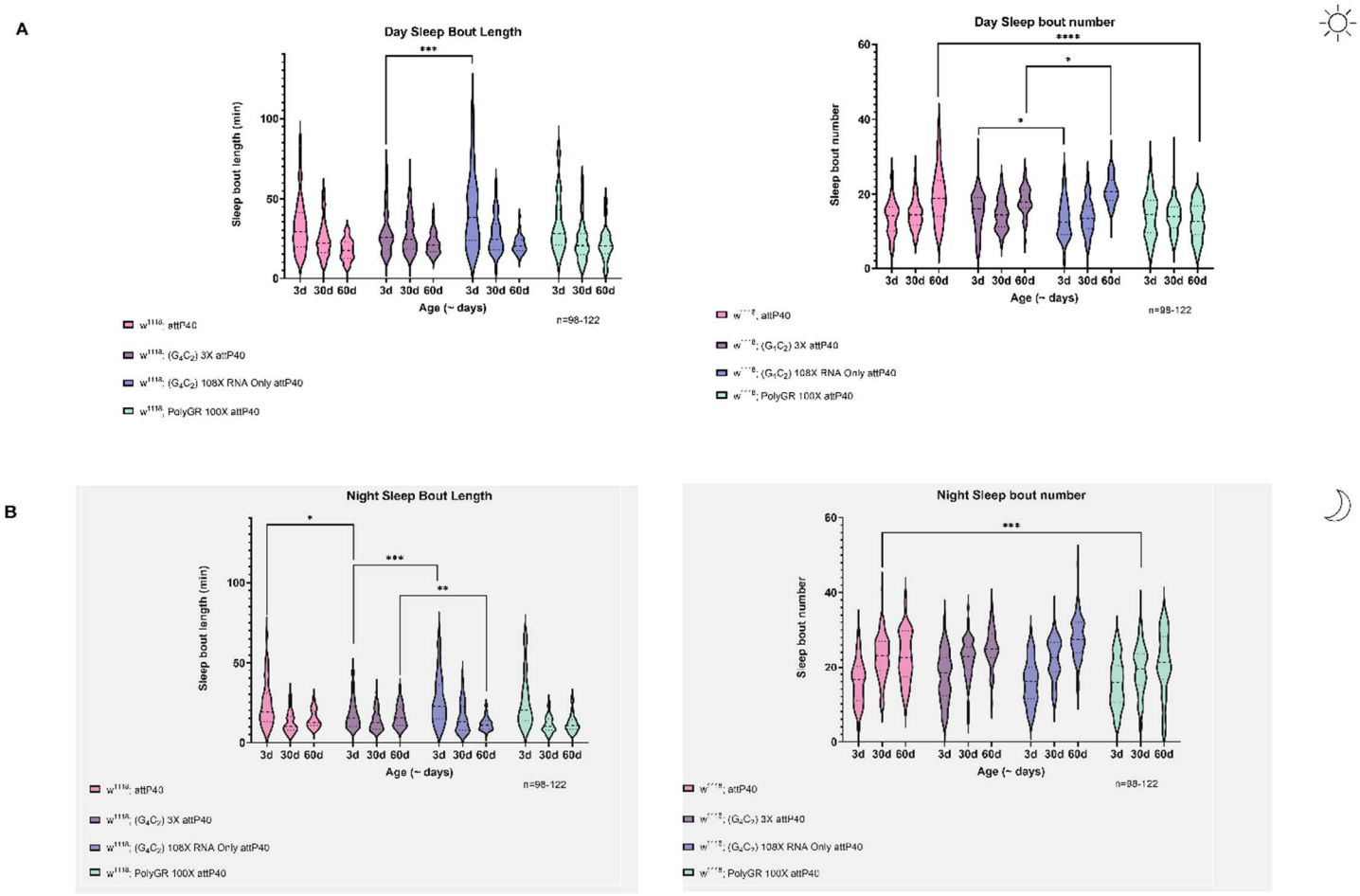

Figure 21. 3-day RNA only HREs (w^{1118}; UAS (G4C2) 108X RO attP40) male flies have an increase in day sleep bout length compared to w^{1118}; UAS (G4C2) 3X attP40 genetic background control (A). Young and middle-aged RNA HREs (w^{1118}; UAS (G4C2) 108X RO attP40) flies have an increase is number of day sleep bouts (A). polyGR repeats (w^{1118}; UAS PolyGR 100X attP40) flies have a significant reduction in day sleep bout number at old age (A). Middle aged RNA only HREs (w^{1118}; UAS (G4C2)108X RO attP40) have a significant increase in night sleep bout length (B). At an older age RNA only HREs (w^{1118}; UAS (G4C2) 108X RO attP40) have a reduction in night sleep bout length (B). PolyGR repeats (w^{1118}; UAS PolyGR 100X attP40) flies have a reduction in night sleep bout number at 30-days (B).

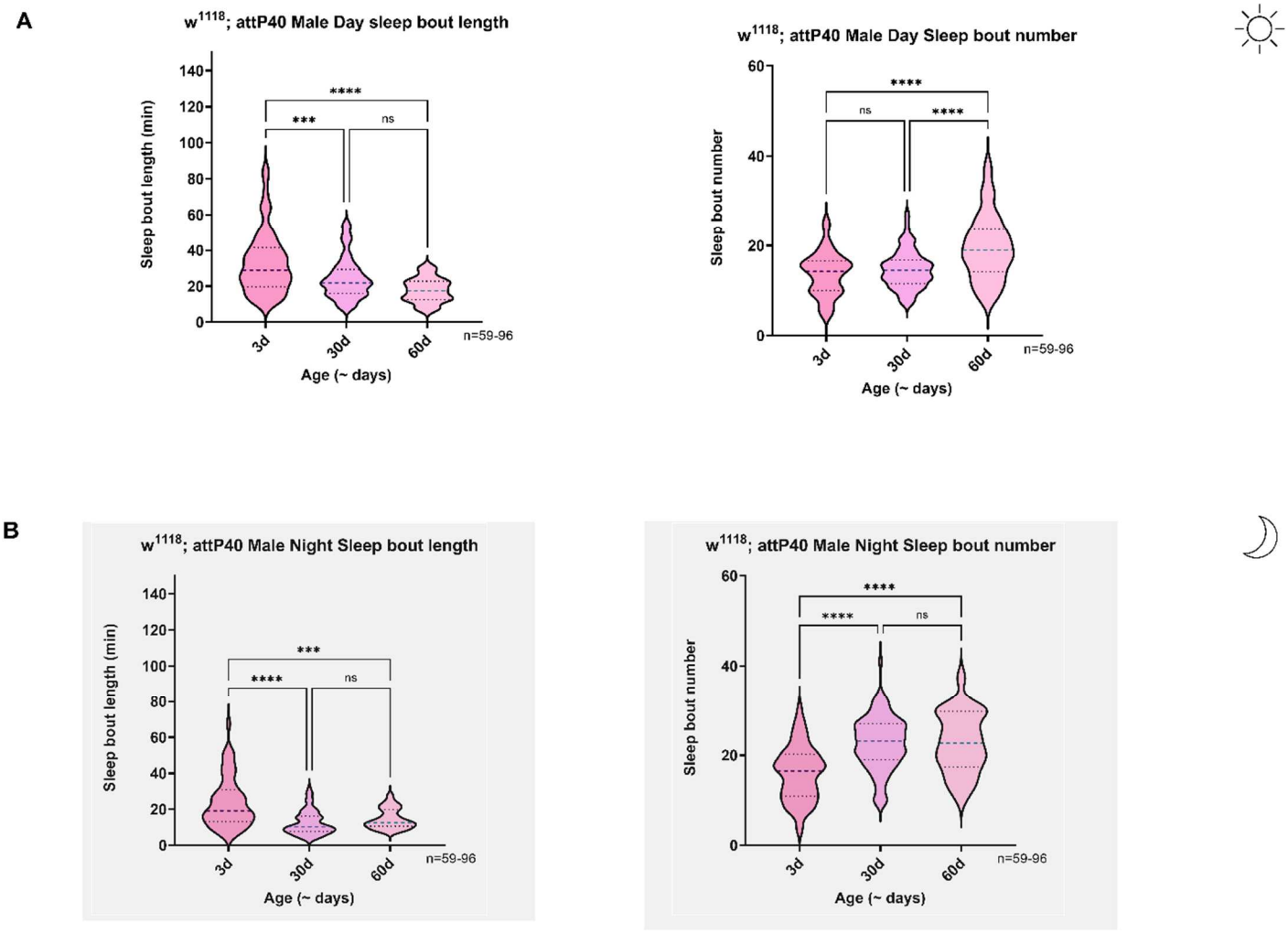

Figure 22. 30-day (w^{1118}; attP40) flies have a significant decrease in day sleep bout length compared to 3-day (A). 60-day (w^{1118}; attP40) flies have a significant decrease in day sleep bout length compared to younger flies (A). Young and middle aged (w^{1118}; attP40) flies have a reduction in day sleep bout number compared to older flies (A). Younger (w^{1118}; attP40) flies have an increase in night sleep bout length compared to middle and older aged flies (B). (w^{1118}; attP40) flies at 3-days have a reduced night sleep bout number compared to middle and older flies (B).

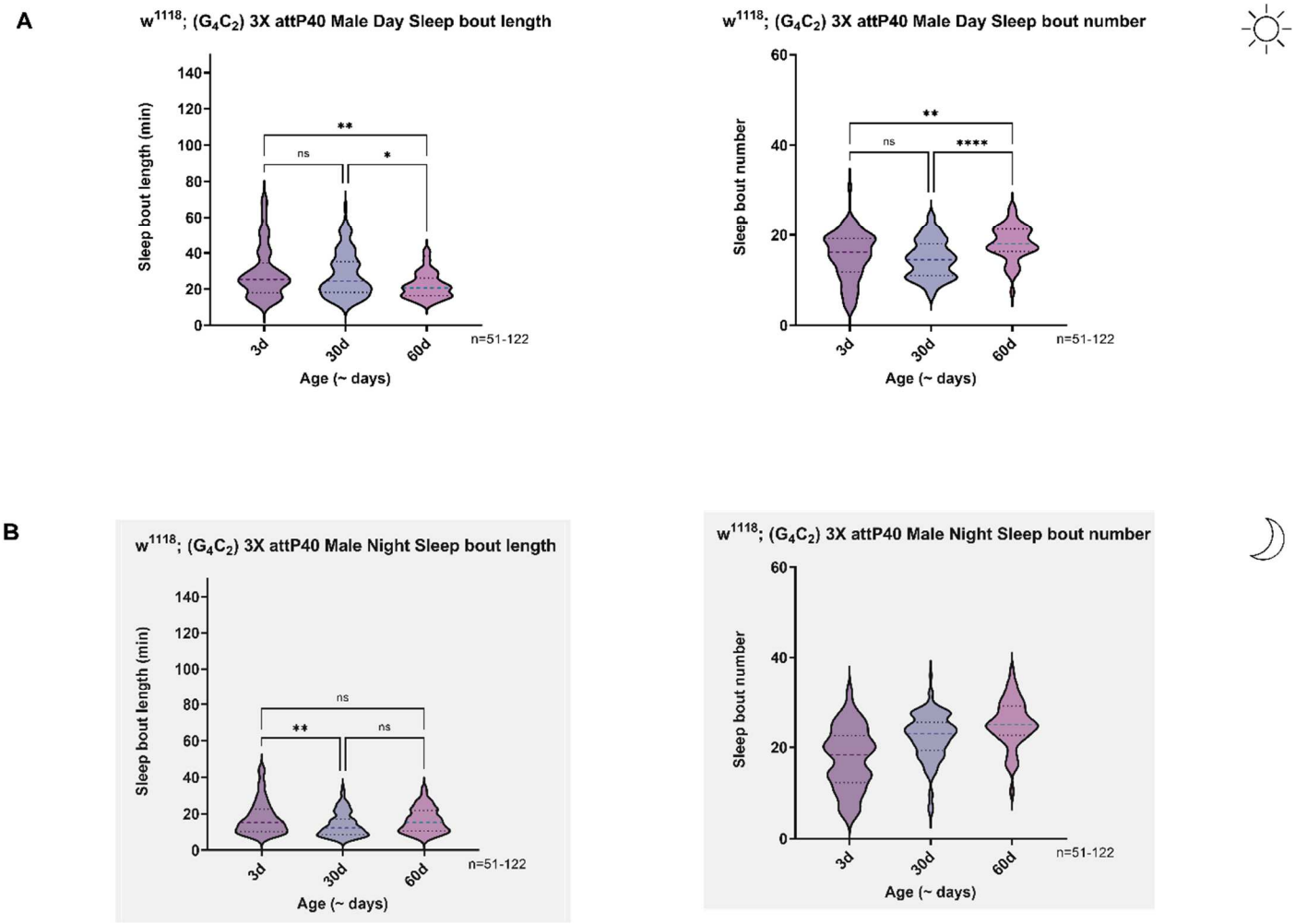

Figure 23. 3-day w^{1118}; UAS (G4C2) 3X attP40 flies show an increase in day sleep bout length compared to 60-day flies (A). 3-day w^{1118}; UAS (G4C2) 3X attP40 flies show an increase in day sleep bout number compared to 60-day flies (A). 3-day w^{1118}; UAS (G4C2) 3X attP40 flies have an increase in night sleep bout length compared to middle aged flies (B).

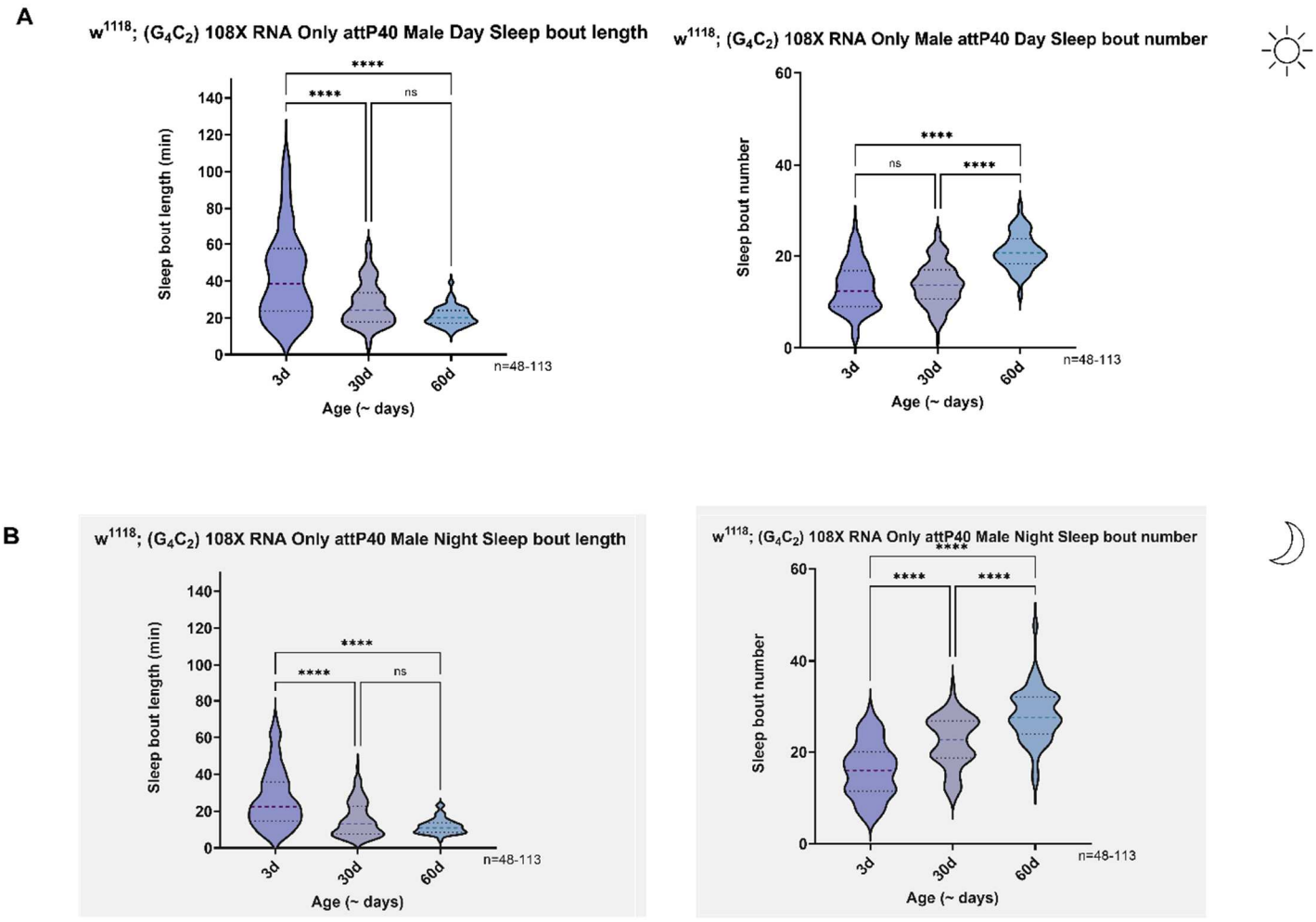

Figure 24. RNA only HREs (w^{1118}; UAS (G4C2) 108X RO attP40) 3-day flies have an increase in day sleep bout length compared to middle and older aged flies (A). RNA only HREs (w^{1118}; UAS (G4C2) 108X RO attP40) 3-day flies have a reduction in day sleep bout number compared to 60-day flies (A). RNA only HREs (w^{1118}; UAS (G4C2) 108X RO attP40) 3-day flies have an increase in night sleep bout length compared to middle and older age points (B).

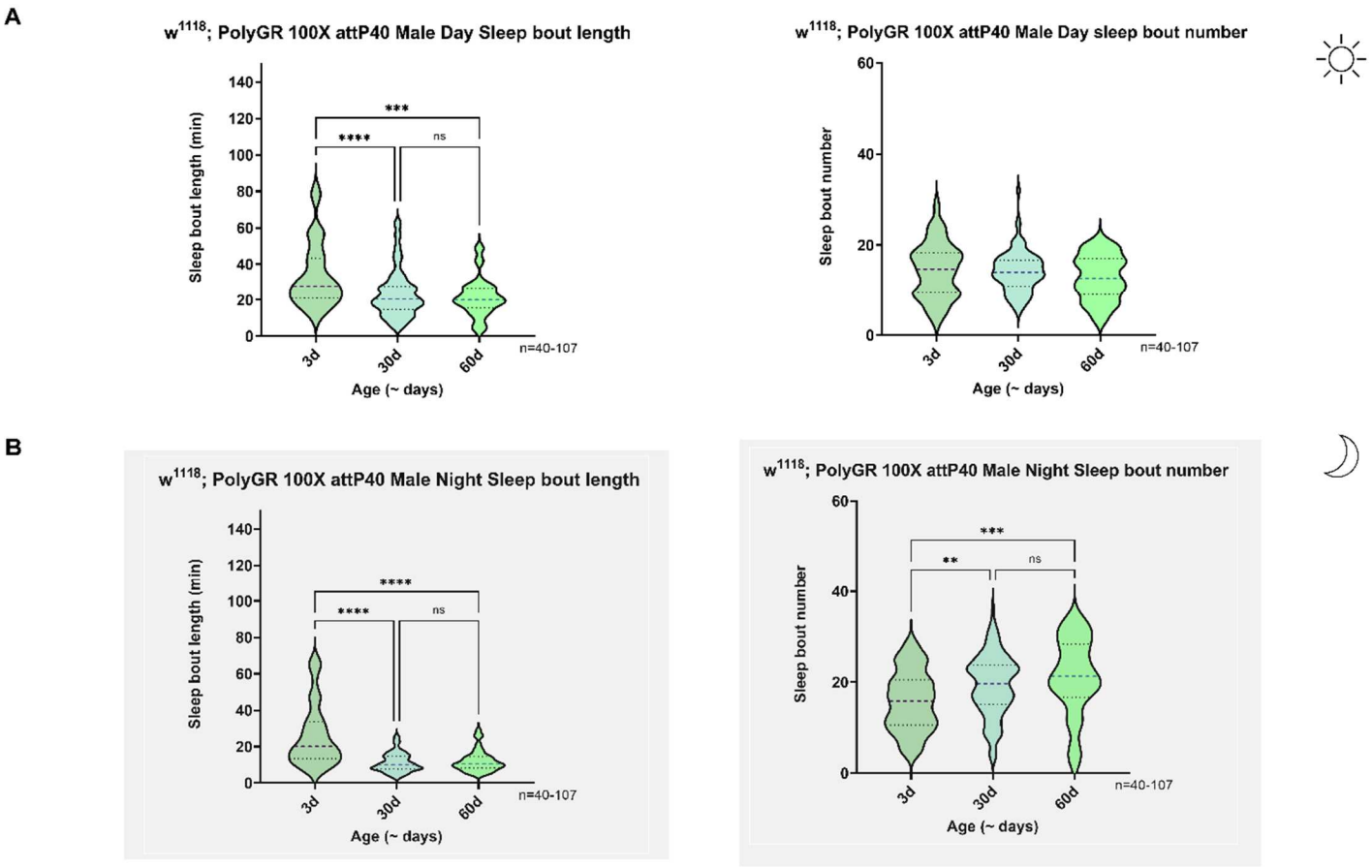

Figure 25. Young polyGR repeats (w^{1118}; UAS PolyGR 100X attP40) flies have an increase in day sleep bout length compared to middle and older flies (A). Young polyGR repeats (w^{1118}; UAS PolyGR 100X attP40) flies have an increase in night sleep bout length compared to older 60-day flies (B). 3-day polyGR repeats (w^{1118}; UAS PolyGR 100X attP40) flies have a reduction in night sleep bout number compared to middle and old aged flies (B).

1A

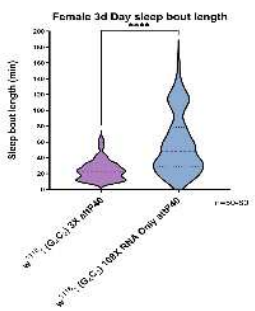

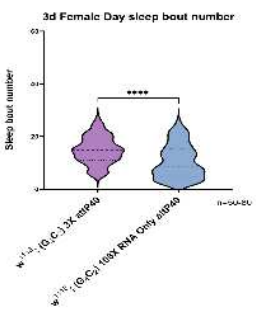

Day Sleep bout length (Right)

Day Sleep bout number (Left)

1B

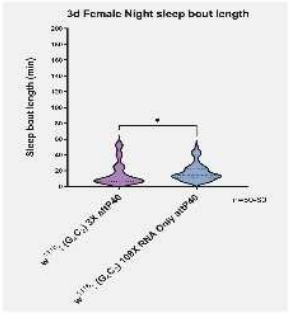

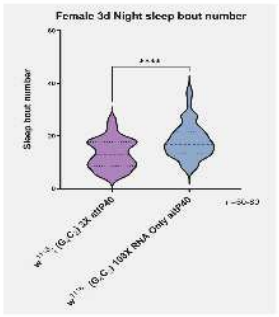

Night Sleep bout length (Right)

Night Sleep bout number (Left)

2A

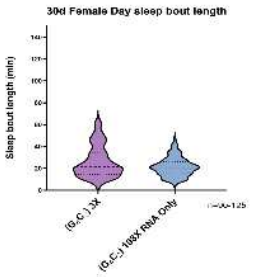

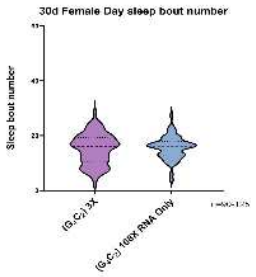

2B

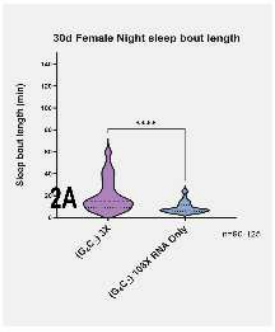

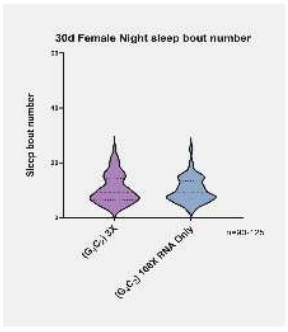

3A

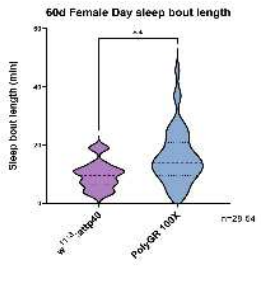

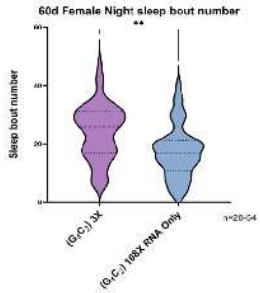

3B

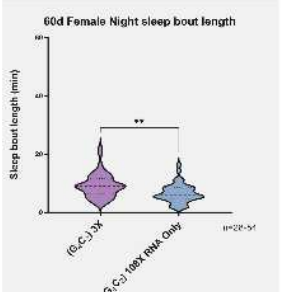

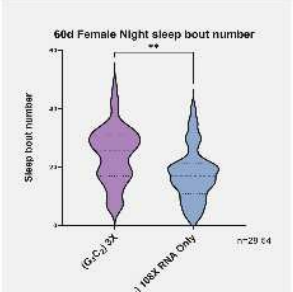

Figure 26. Female RNA only HREs (w^{1118}; UAS (G4C2) 108X RO attP40) flies have an increase in day sleep bout length and number at 3-days (1A). RNA only HREs (w^{1118}; UAS (G4C2) 108X RO attP40) flies have a significant increase in night sleep bout number and a slight decrease in sleep bout length (1B). Middle aged RNA only HREs (w^{1118}; UAS (G4C2) 108X RO attP40) flies have a reduction in day and night sleep bout length (2B). Old, aged RNA only HREs (w^{1118}; UAS (G4C2) 108X RO attP40) flies show an increase in day sleep bout length (3A). While they have a decrease in day and night sleep bout number (3A-3B). 60-day aged RNA only HREs (w^{1118}; UAS (G4C2) 108X RO attP40) flies show a decrease in night sleep bout length compared to their (w^{1118}; UAS (G4C2) 3X attP40) genetic background control (3B).

1A

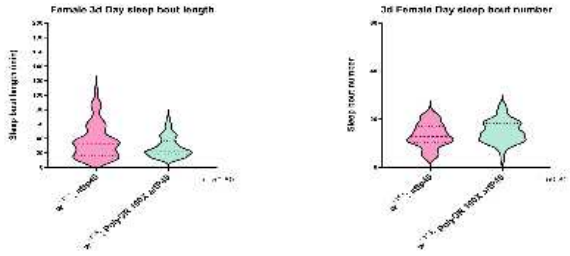

☼

Day Sleep bout length (Right)

Day Sleep bout number (Left)

1B

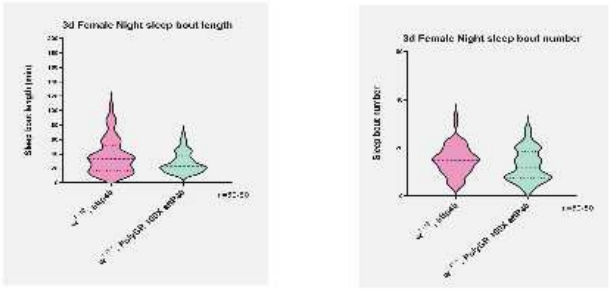

☽

Night Sleep bout length (Right)

Night Sleep bout number (Left)

2A

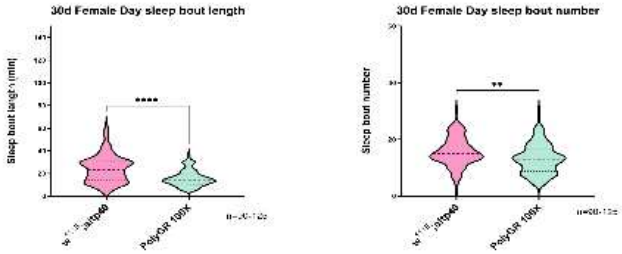

2B

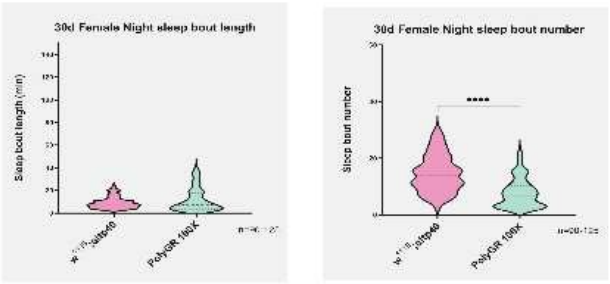

3A

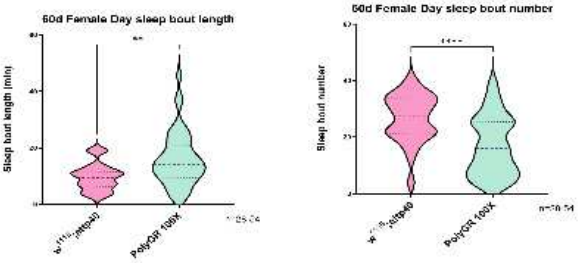

3B

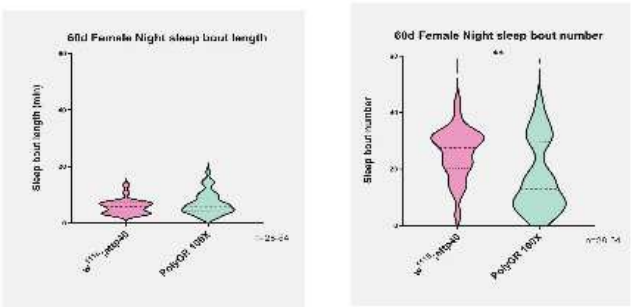

Figure 27. polyGR repeats (w^{1118}; UAS PolyGR 100X attP40) flies exhibit a significant decline in day sleep bout length with an increase in sleep bout number at 30 days old (1A). On the other hand, 30-day flies show an increase in night sleep bout length and a decrease in sleep bout number (2B). 60-day polyGR repeats (w^{1118}; UAS PolyGR 100X attP40) present an increase in day sleep bout length and number and a significant increase in night sleep bout length compared to genetic background controls (w^{1118}; attP40) (3A-3B).day sleep bout length and number and a

significant increase in night sleep bout length compared to genetic background controls (w^{1118}; attP40) (3A-3B).

1A

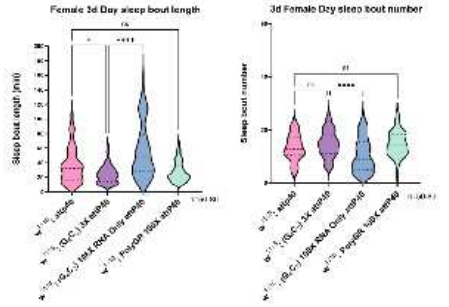

Day Sleep bout length (Right)

Day Sleep bout number (Left)

1B

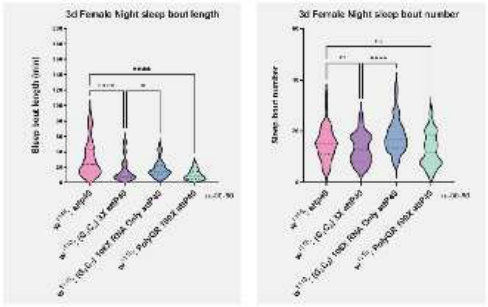

Night Sleep bout length (Right)

Night Sleep bout number (Left)

2A

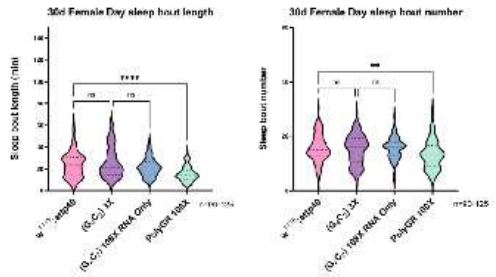

2B

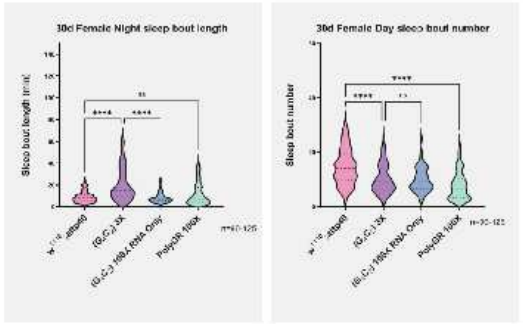

3A

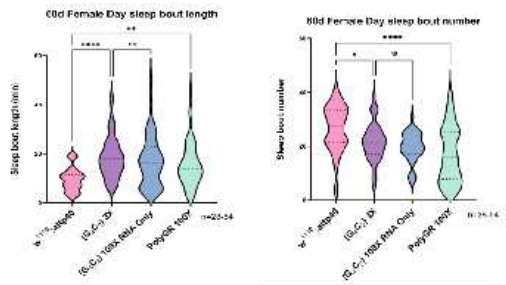

3B

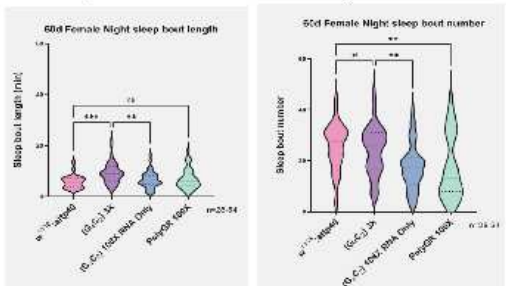

Figure 28. Female RNA only HREs (w^{1118}; UAS (G4C2) 108X RO attP40) flies have an increase in day sleep bout length and number at 3-days (1A). RNA only HREs (w^{1118}; UAS (G4C2) 108X RO attP40) flies have a significant increase in night sleep bout number (1B). 3-day polyGR repeats (w^{1118}; UAS PolyGR 100X attP40) flies exhibit a significant reduction in night sleep bout length (1B). Middle aged RNA only HREs (w^{1118}; UAS (G4C2) 108X RO attP40) flies have a reduction in day and night sleep bout length (2B). 30-day polyGR repeats (w^{1118}; UAS PolyGR 100X attP40) flies exhibit a reduction in day sleep bout length (2A). In contrast, polyGR repeats (w^{1118}; UAS PolyGR 100X attP40) flies show an increase in day and night sleep bout number (2A-2B). And an increase in night sleep bout length (2B). 60-day polyGR repeats (w^{1118}; UAS PolyGR 100X attP40) flies display an increase in day sleep bout number and length (3A). And an increase in night sleep bout number and length (3B). Old, aged RNA only HREs (w^{1118}; UAS (G4C2) 108X RO attP40) show an increase in day sleep bout length (3A). While they have a decrease in day and night sleep bout number (3A-3B). 60-day aged RNA only HREs (w^{1118}; UAS (G4C2) 108X RO attP40) flies show a decrease in night sleep bout length (3B).

Table 8. Summary of female day sleep demonstrating that 3-day RNA only HREs (w^{1118}; UAS (G4C2) 108X RO attP40) flies have an increase in sleep bout length and reduction in sleep bout number. Older RNA only HREs (w^{1118}; UAS (G4C2) 108X RO attP40) flies have an increase in sleep bout length, but no change in bout number. Additionally, polyGR repeats (w^{1118}; UAS PolyGR 100X attP40) show an overall decrease in sleep at middle age genetic background control (w^{1118}; attP40). In stark contrast, older polyGR repeats (w^{1118}; UAS PolyGR 100X attP40) flies show an increase in sleep during the day.

Genotype	**Age (days)**	**Phenotype**
w^{1118}; attP40	3	None
w^{1118}; attP40	30	None

w^{1118}; attP40	60	None
w^{1118}; UAS (G4C2) 3X attP40	3	Sleep bout length: Decrease Sleep bout number: Increase
w^{1118}; UAS (G4C2) 3X attP40	30	None
w^{1118}; UAS (G4C2) 3X attP40	60	Sleep bout length: Decrease Sleep bout number: No change
w^{1118}; UAS (G4C2) 108X RO attP40	3	Sleep bout length: Increase Sleep bout number: Decrease
w^{1118}; UAS (G4C2) 108X RO attP40	30	None

w^{1118}; UAS (G4C2) 108X RO attP40	60	Sleep bout length: Increase Sleep bout number: None
w^{1118}; UAS PolyGR 100X attP40	3	None
w^{1118}; UAS PolyGR 100X attP40	30	Sleep bout length: Decrease Sleep bout number: Decrease
w^{1118}; UAS PolyGR 100X attP40	60	Sleep bout length: Increase Sleep bout number: Increase

Table 9. Summary of female night sleep results demonstrating RNA only HREs (w^{1118}; UAS (G4C2) 108X RO attP40) a reduction in sleep bout length at each age point compared to its control (w^{1118}; UAS (G4C2) 3X attP40). At 30 days polyGR repeats (w^{1118}; UAS PolyGR 100X attP40) flies have a reduction in sleep bout number, but an increase in sleep bout number at 60 days.

Genotype	**Age (days)**	**Phenotype**

w^{1118}; attP40	3	None
w^{1118}; attP40	30	None
w^{1118}; attP40	60	None
w^{1118}; UAS (G4C2) 3X attP40	3	Sleep bout length: Increase Sleep bout number: Decrease
w^{1118}; UAS (G4C2) 3X attP40	30	Sleep bout length: Increase Sleep bout number: No change
w^{1118}; w^{1118}; UAS (G4C2) 3X attP40	60	Sleep bout length: Decrease Sleep bout number: Decrease

w^{1118}; UAS (G4C2) 108X RO attP40	3	Sleep bout length: Decrease Sleep bout number: Increase
w^{1118}; UAS (G4C2) 108X RO attP40	30	Sleep bout length: Decrease Sleep bout number: No change
w^{1118}; UAS (G4C2) 108X RO attP40	60	Sleep bout length: Decrease Sleep bout number: Decrease
w^{1118}; UAS PolyGR 100X attP40	3	None
w^{1118}; UAS PolyGR 100X attP40	30	Sleep bout length: No change Sleep bout number: Decrease
w^{1118}; UAS PolyGR 100X attP40	60	Sleep bout length: No change Sleep bout number: Increase

Female sleep across lifespan

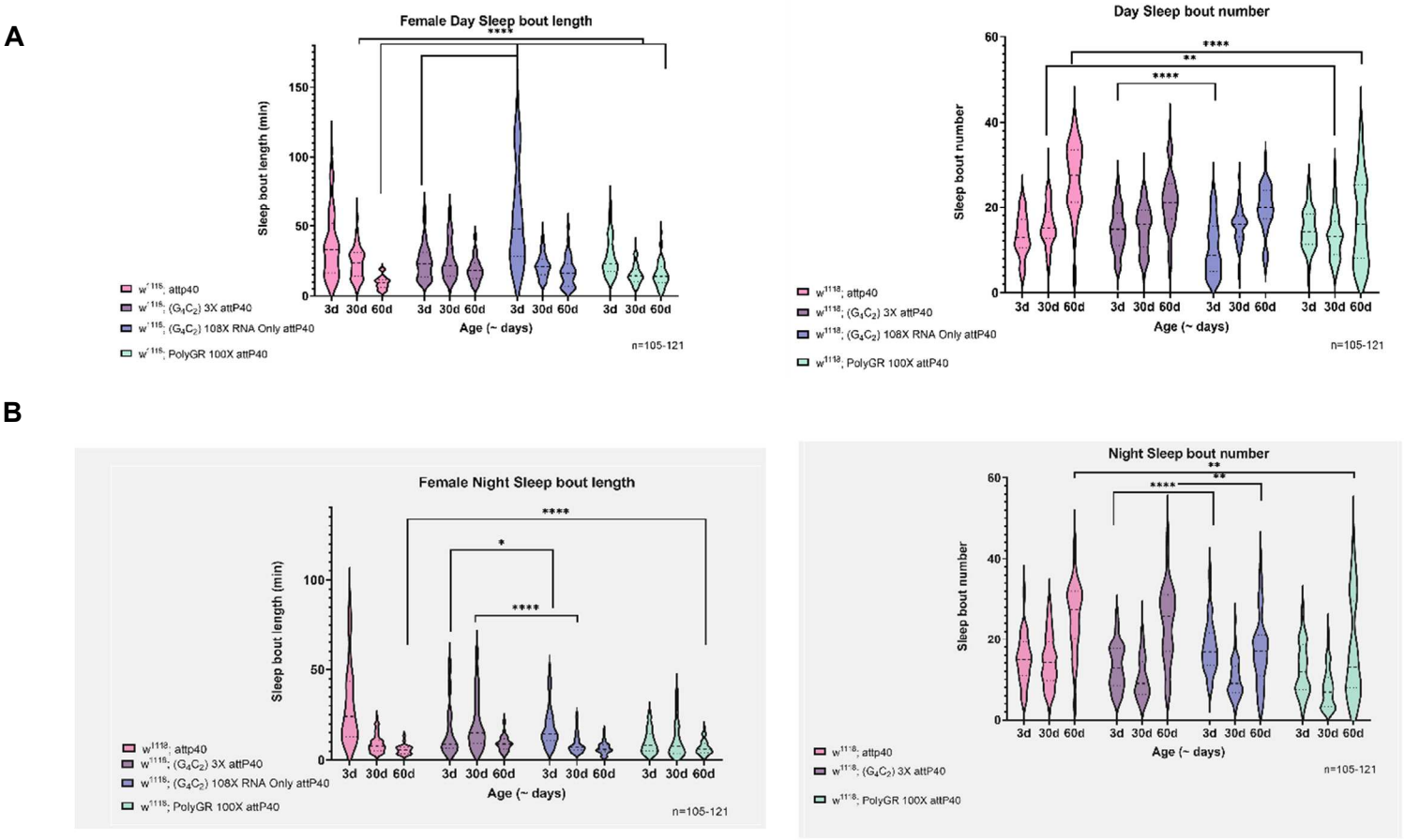

Figure 29. 3-day RNA only HREs (w^{1118}; UAS (G4C2) 108X RO attP40) flies have an increase in day sleep bout length (A). 30 and 60-day polyGR repeats (w^{1118}; UAS PolyGR 100X attP40) flies have an increase in day sleep bout number compared to 3-day flies (A). 3-day RNA only HREs (w^{1118}; UAS (G4C2) 108X RO attP40) flies have a reduction in day sleep bout number (A). 3-day RNA only HREs (w^{1118}; UAS (G4C2) 108X RO attP40) flies have a decrease in night sleep bout length (B). (B). 3-day RNA only HREs (w^{1118}; UAS (G4C2) 108X RO attP40) flies have an increase in night sleep bout number (B).

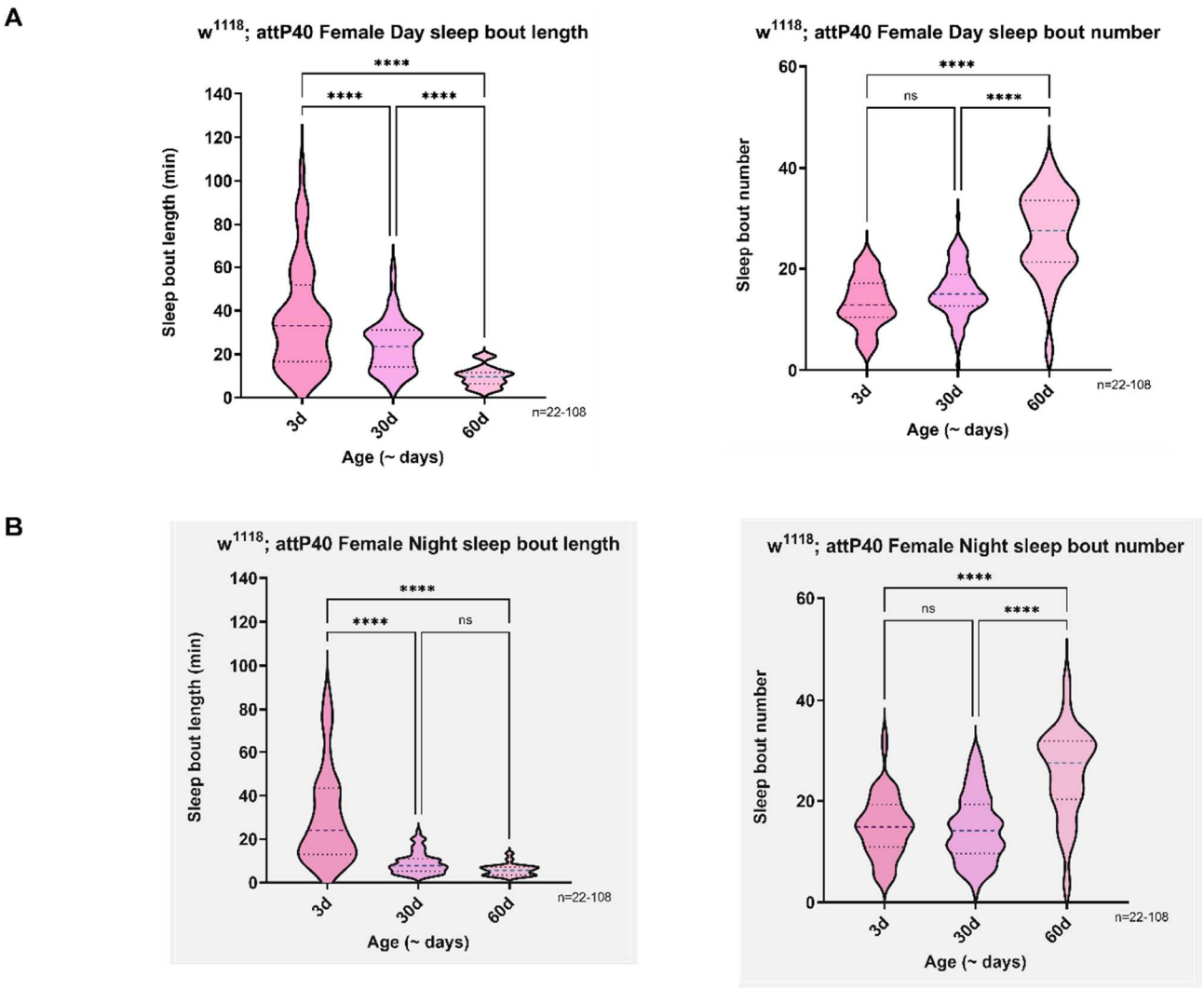

Figure 30. 3-day (w^{1118}; attP40) flies show an increase in day and night sleep bout length compared to middle and older aged flies. 60-day (w^{1118}; attP40) flies have an increase in night sleep bout number compared to young flies.

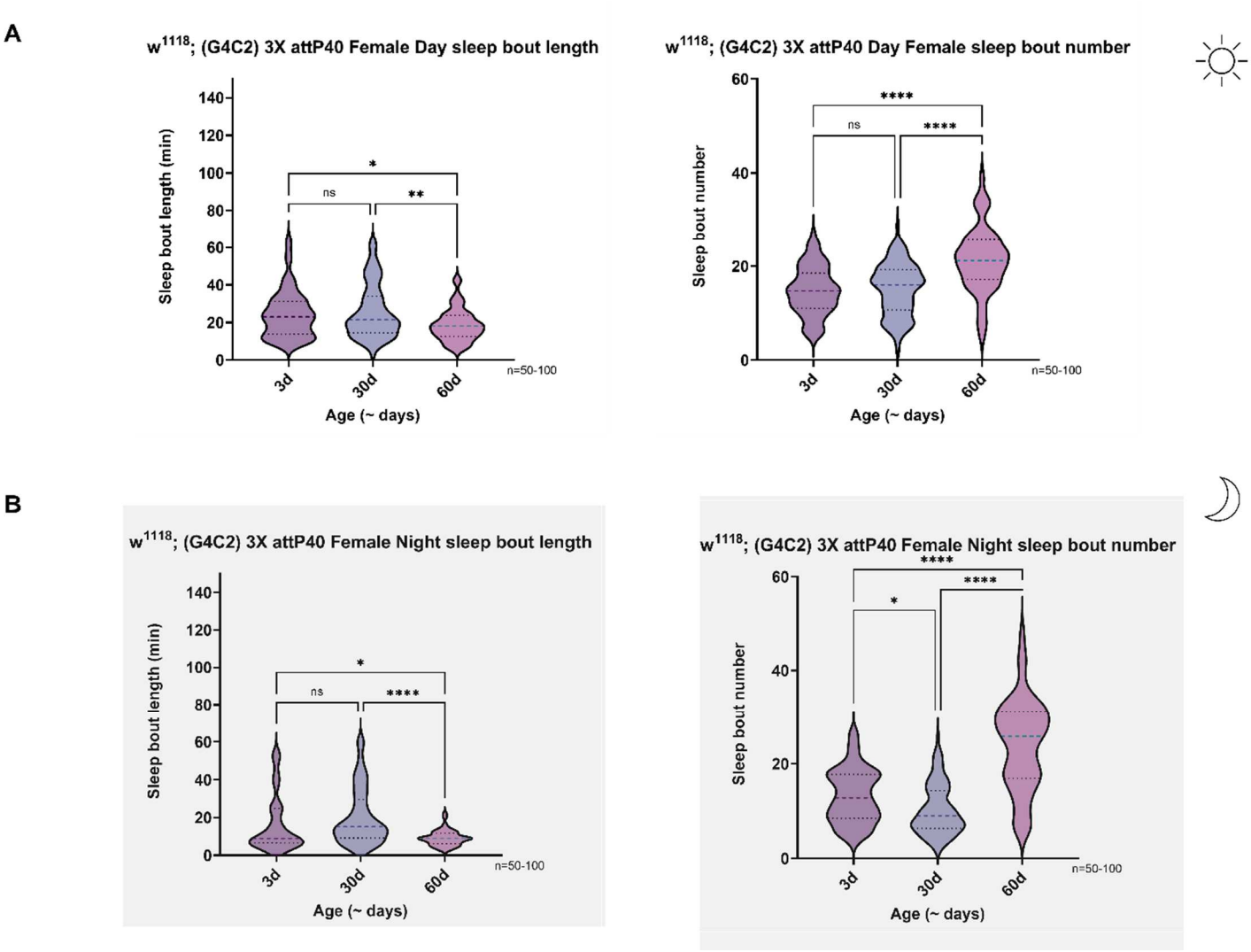

Figure 31. (w^{1118}; UAS (G4C2) 3X attP40) 60-day flies have a reduction in day and night sleep bout length compared to 3-day flies. Old aged (w^{1118}; UAS (G4C2) 3X attP40) flies have an increase in day and night sleep bout number compared to 3-day flies.

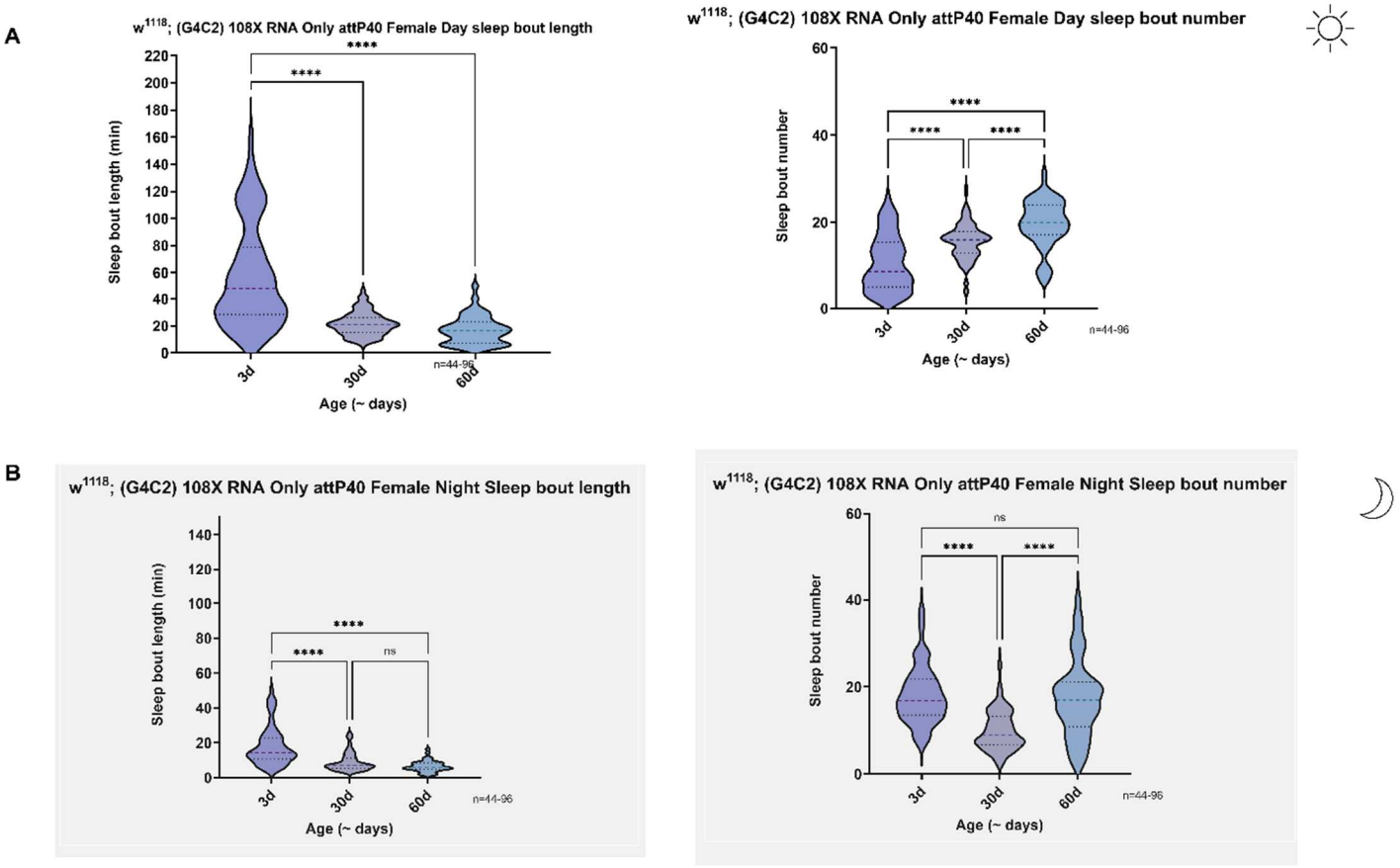

Figure 32. Young RNA only HREs (w^{1118}; UAS (G4C2) 108X RO attP40) flies have an increase in day sleep bout length compared to middle and old aged flies (A). 60-day RNA only HREs (w^{1118}; UAS (G4C2) 108X RO attP40) flies have a significant reduction in night sleep bout length compared to young flies (B).

A

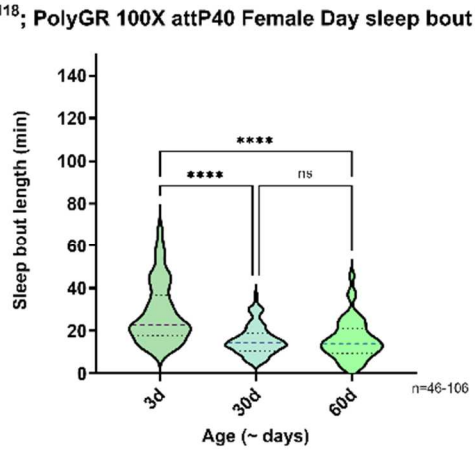

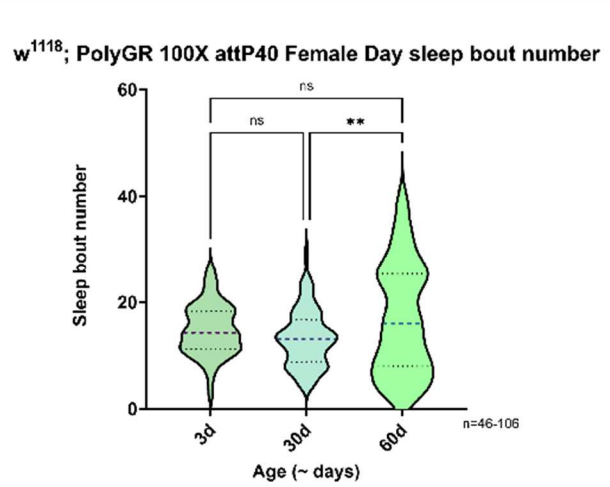

B

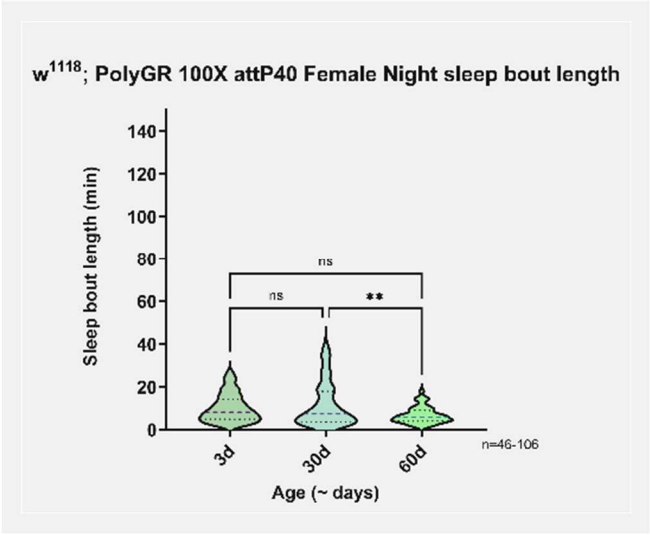

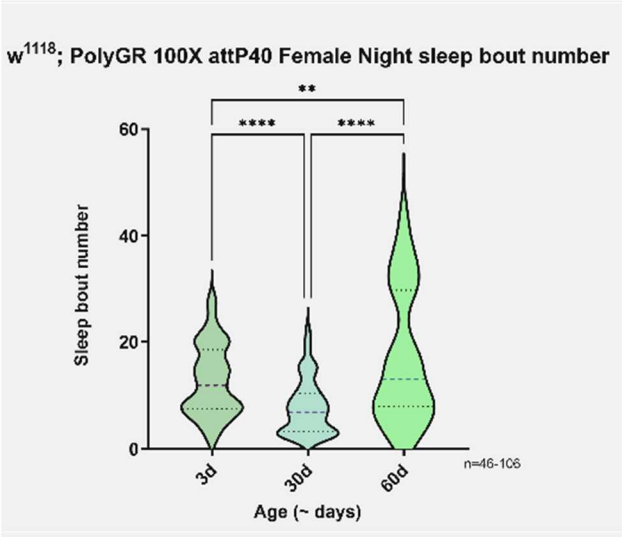

Figure 33. 3-day polyGR repeats (w^{1118}; UAS PolyGR 100X attP40) flies have an increase in day sleep bout number (A). 30-day polyGR repeats (w^{1118}; UAS PolyGR 100X attP40) flies have a reduction in day sleep bout number compared to young flies (A). 30-day polyGR repeats (w^{1118}; UAS PolyGR 100X attP40) flies have a reduction in night sleep bout number compared to young flies (B).

Overexpression of C9orf72 HREs and polyGR DPRs cause age dependent axonal degeneration in MBs

Neuroimaging in human brain tissue has been performed to observe the underlying impact of C9orf72 expansion on brain morphology in particular (G_4C_2) hexanucleotide repeats have been found in the frontal cortex in FTD patient brain tissues (Renton *et al.*, 2011). Another research study uncovered that the number of C9orf72 hexanucleotide correlated with frontal lobe in cases of FTD (Shaw and Kirby, 2014). The mushroom body region of the Drosophila brain is responsible for many behavioral FTD phenotypes including olfactory learning and memory, decision making, sleep regulation, appetite, and social behavior (Pitman *et al.*, 2006);(Turner *et al.*, 2008);(Zhu, 2020);(Chen-Han and Lin, 2018). Previous studies in Drosophila models of Alzheimer's disease Tau protein induced neurodegeneration were validated using Anti-Fasciclin-II antibodies as a marker for mushroom body neurons (Gistelinck *et al.*, 2012). Our study used Anti-Fasciclin-II to better understand morphological changes in mushroom body anatomy in a Drosophila model of C9orf72 expression.

Our preliminary study concluded that polyGR repeats (w^{1118}; UAS PolyGR 100X attP40) flies exhibited significant reduction in MB lobe length and width compared to genetic background control (w^{1118}; attP40) at middle and old age. Furthermore, RNA only HREs (w^{1118}; UAS (G4C2) 108X RO attP40) flies displayed a decrease in γ lobe width at 60-days. Visually apparent changes in Anti-Fasciclin-II (marker for MB neurons (Gistelinck *et al.*, 2012)) signal intensity were observed in 60-day flies across genotypes making it difficult to quantify lobe thinning.

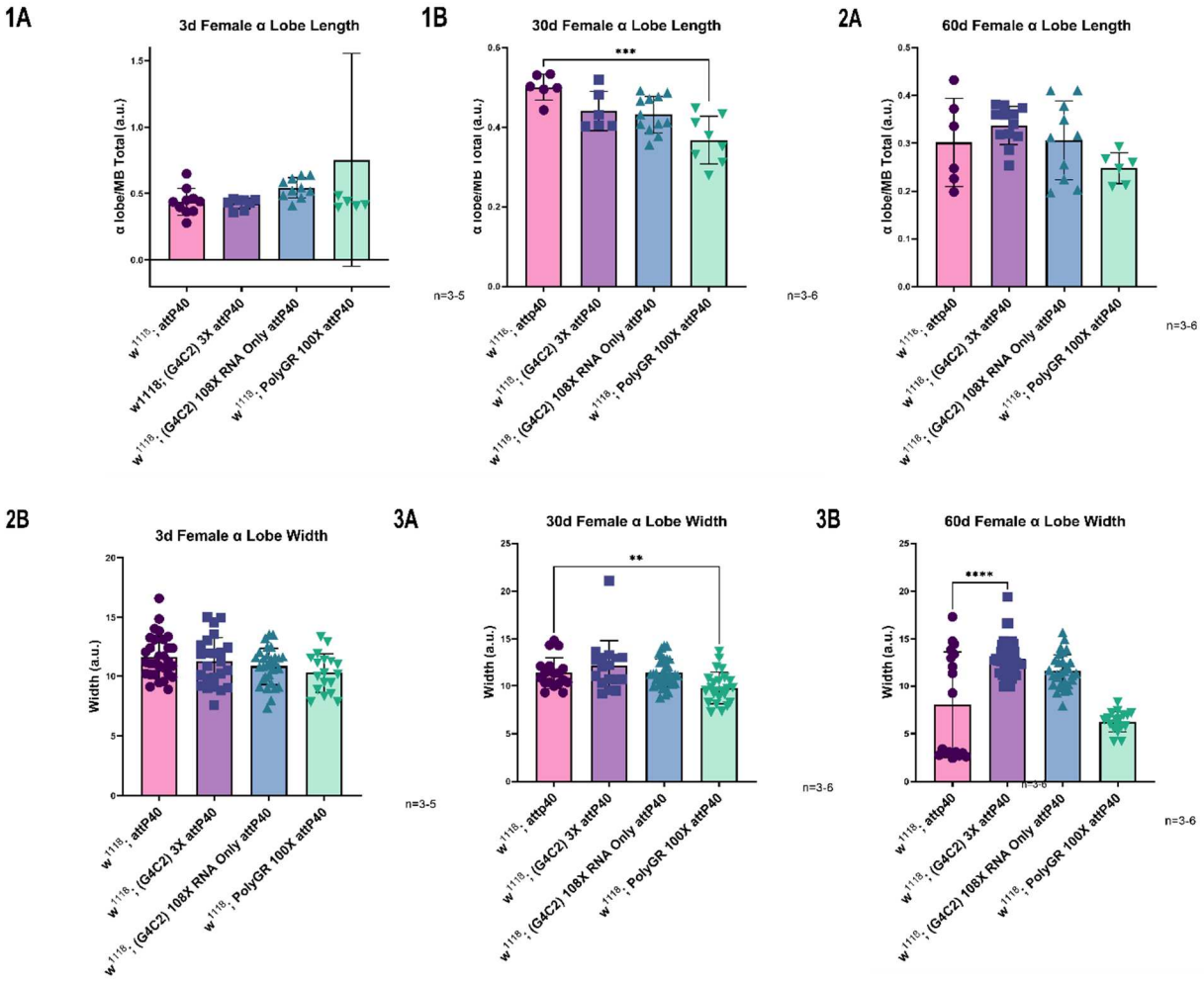

Figure 34. Both middle and older aged polyGR repeats (w^{1118}; UAS PolyGR 100X attP40) flies showed a reduction in α lobe length and width compared to their genetic background controls (w^{1118}; attP40) (1B and 3B).

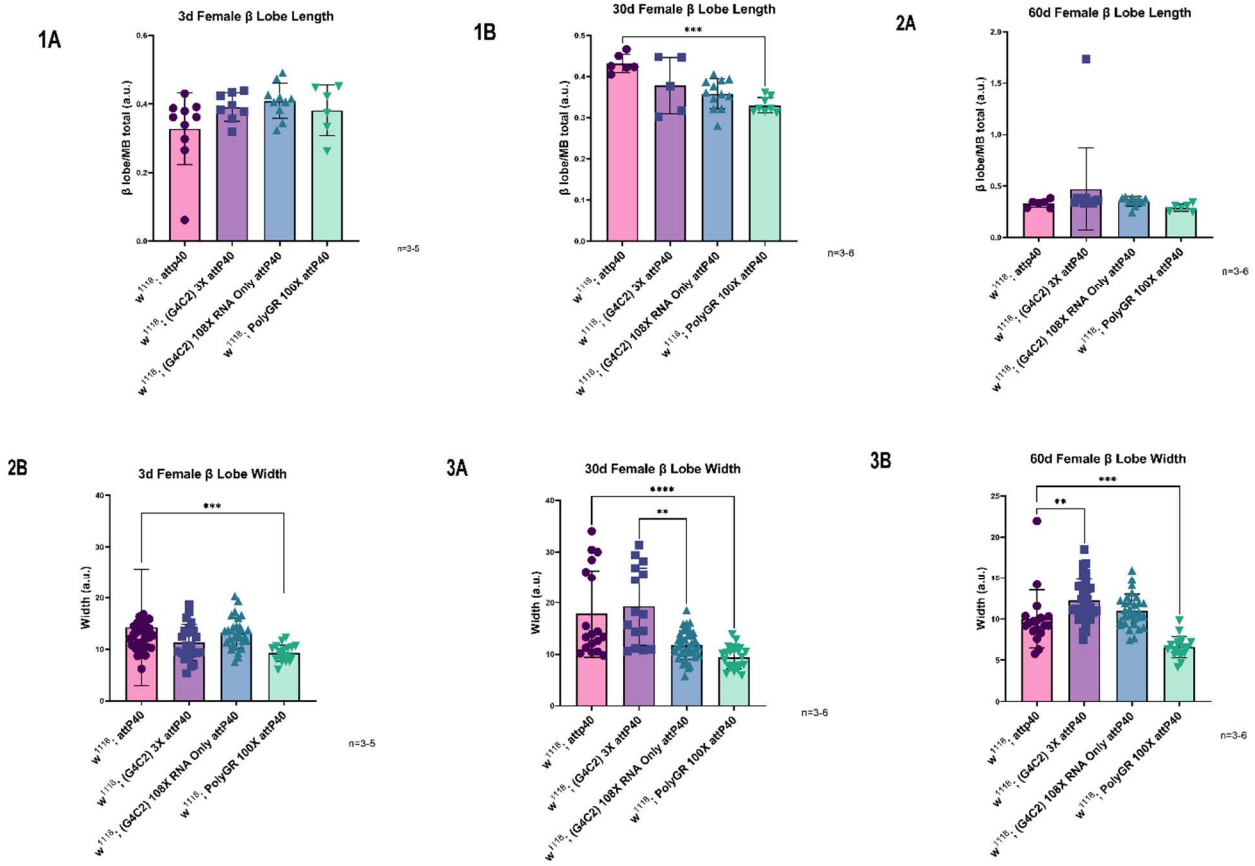

Figure 35. Middle and old aged polyGR repeats (w^{1118}; UAS PolyGR 100X attP40) flies showed a reduction in β lobe length and width (1B and 3A-3aB).

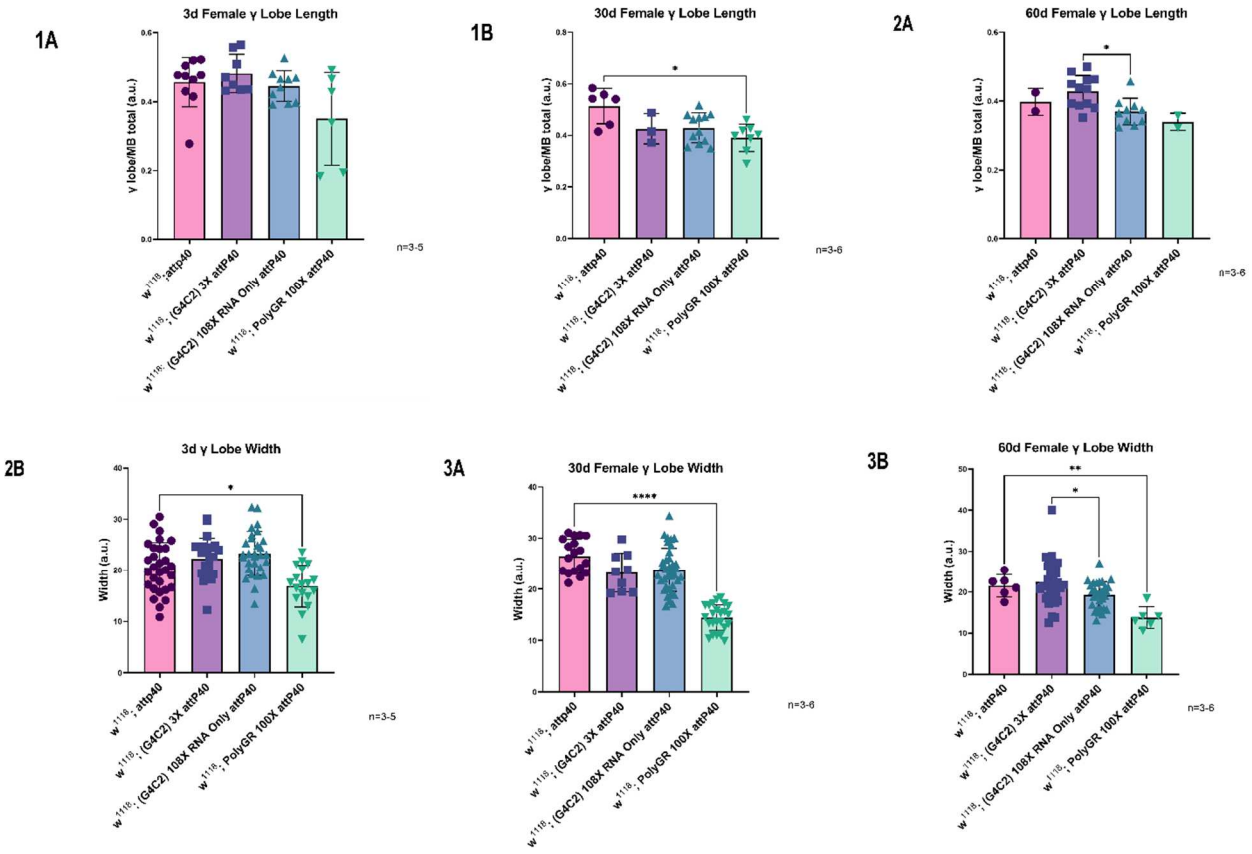

Figure 16. At 30-days polyGR repeats (w^{1118}; UAS PolyGR 100X attP40) flies displayed a reduction in γ lobe length and width (1B and 3A). Additionally, at 60-days both RNA only HREs (w^{1118}; UAS (G4C2) 108X RO attP40) and polyGR repeats (w^{1118}; UAS PolyGR 100X attP40) flies exhibited a significant reduction in γ lobe length and width (2A and 3B).

Discussion

The present findings in this study show that overexpression of C9orf72 HREsand DPRs in Drosophila MBs cause FTD like phenotypes. Sleep studies revealed that young RNA only HRE flies exhibited greater sleepiness, while polyGR repeat flies displayed sleep changes later in their lifespan. Old (60 day) RNA only HRE expressing males showed sleep fragmentation while female flies exhibited greater sleepiness. Additionally, old polyGR expressing male flies are more active during the day while their female counterparts are less active. Overall, during middle and old age RNA only HREs and polyGR repeat flies presented changes in their sleep patterns compared to their genetic background controls. Y-Maze results uncovered that there were changes in both RNA only HREs and polyGR repeat distanced moved. This finding indicates possible hyperactivity in C9orf72 hexanucleotide repeat expansion flies through an increase in movement at both young and old age points. However, when we normalized percent alternation to the fly's total distance moved no differences were observed across genotypes or during lifespan. This assay shows that although the flies may show changes in alternation, the impact of C9orf72 on working memory is confounded by changes in movement, in both an age and genotype dependent manner. ;For example, in our results that we collected we have parameters

that could measure the fly's latency to decide, cumulative duration for the amount of time the fly was moving in the center, and the frequency of the fly moving in the center of the maze. Lastly, MB morphology studies discovered that polyGR repeat flies exhibit significant MB lobe thinning starting at a young age suggesting that polyGR DPR species affect axonal integrity early on during lifespan. Additionally, RNA only HREs flies showed γ lobe thinning in old age. Overall, polyGR DPRs display both genotype and age-related neurodegeneration starting at a young age whereas, RNA HREs flies show neurodegeneration at older ages beginning with γ lobe thinning.

Modeling FTD disease pathology in *Drosophila* can provide us insights into how C9orf72 HREs or DPR pathology works at a cellular level in an intact organism. By characterizing FTD relevant phenotypes using behavioral assays to test the fly's working memory, sleep, and neurodegeneration we can better understand the basis of complex FTD symptoms in humans. Knowing that behavioral FTD can be diagnosed with working memory, sleep, and neurodegeneration features we chose a *Drosophila* model where C9orf72 HREs or DPRs were expressed specifically in the MB region of the fly's brain. MB neurons have been shown in previous studies to control learning, memory, decision making, sleep regulation, appetite, and social behaviors Allada (2006); Laurent (2008); Zhu (2020); Lin (2018). By using this model of C9orf72 induced FTD in *Drosophila* we were able to better understand whether this model would be useful to further uncover the molecular mechanisms behind FTD sleep regulation, working memory, and MB lobe thinning. This study allows us to conclude that both C9orf72 HREs and DPRs flies exhibit sleep dysregulation, hyperactivity, and MB lobe thinning changes that could be examined closer to determine the underlying mechanisms of disease and provide further information on the genetic pathways and cellular mechanisms behind C9orf72 induced FTD.

Acknowledgements

The completion of this study would have not been possible without the contributions of the "Genotypic and phenotypic examination of disease pathogenesis in C9orf72 FTD" study funding through the U.S Department of Defense grant W81XWH1910276 (DoD, Sattler, R and Jensen, K (co-PIs), D Zarnescu sub-award PI).

References

A., N.J.C.E.H.B.I.R., M., M.M.N.V., Kimmo, Y.L., Hatanpaa, J., and Mann, D.M.A. (2007). Neuropathologic diagnostic and nosologic criteria for frontotemporal lobar degeneration: consensus of the Consortium for Frontotemporal Lobar Degeneration. Acta Neuropathologica *114*, 5-22.

Aso, Y., Hattori, D., Yu, Y., Iyer, R.M.J.N.A., Ngo, T.-T., Dionne, H., Abbott, L., and Axel, R. (2014). The neuronal architecture of the mushroom body provides a logic for associative learning. eLife. 10.7554/eLife.04577.

Baker, M., Mackenzie, I.R., Pickering-Brown, S.M., Gass, J., Rademakers, R., Lindholm, C., Snowden, J., Adamson, J., Sadovnick, A.D., Rollinson, S., et al. (2006). Mutations in progranulin cause tau-negative frontotemporal dementia linked to chromosome 17. Nature Communications *442*, 916-919.

Beck, J., Poulter, M., Hensman, D., Rohrer, J.D., Mahoney, C.J., Adamson, G., Campbell, T., Uphill, J., Borg, A., Fratta, P., et al. (2013). Large C9orf72 hexanucleotide repeat expansions are seen in multiple neurodegenerative syndromes and are more frequent than expected in the UK population. American journal of human genetics *92*, 342-353.

Braak, H., and Braak, E. (1987). Argyrophilic grains: characteristic pathology of cerebral cortex in cases of adult onset dementia without Alzheimer changes. Neuroscience Letters *76*, 124-127.

Braems, E., Swinnen, B., and Van Den Bosch, L. (2020). C9orf72 loss-of-function: a trivial, stand-alone or additive mechanism in C9 ALS/FTD? Acta Neuropathologica *140*, 625-643.

Chen-Han, C.-H.C.-C.C., and Lin, L.H.-Y.Y.S. (2018). *Drosophila* mushroom bodies integrate hunger and satiety signals to control innate food-seeking behavior. Neuroscience.

Cichewicz, K., and Hirsh, J. (2018). ShinyR-DAM: a program analyzing *Drosophila* activity, sleep, and circadian rhythms. Communications Biology. 10.1038/s42003-018-0031-9.

Ciura, S., Lattante, S., Ber, I.L., Latouche, M., Tostivint, H., Brice, A., and Kabashi, E. (2013). Loss of function of C9orf72 causes motor deficits in a zebrafish model of amyotrophic lateral sclerosis. Annals of neurology *74*, 180-187.

Colby (2020). Projections of the Size and Composition of the U.S. Population: 2014 to 2060. Population Estimates and Projections. 2020 Alzheimer's disease facts and figures. Alzheimer's Association Report.

Dong, W., Zhang, L., Sun, C., Gao, X., and Zhang, L. (2020). Knock in of a hexanucleotide repeat expansion in the C9orf72 gene induces ALS in rats Animal models and experimental medicine *3*, 237-244.

Economou, N.-T., Paparrigopoulos, T., Bonanni, E., Maestri, M., Carnicelli, L., Coscio, E.D., Ktonas, P., Vagiakis, E., and Papageorgiou, P.T.S.G. (2014). Sleep in frontotemporal dementia is equally or possibly more disrupted, and at an earlier stage, when compared to sleep in Alzheimer's disease. Journal of Alzheimer's Disease.

Gijselinck, I., Van Langenhove, T., van der Zee, J., Sleegers, K., Philtjens, S., Kleinberger, G., Janssens, J., Bettens, K., Van Cauwenberghe, C., Pereson, S., et al. (2012). A C9orf72 promoter repeat expansion in a Flanders-Belgian cohort with disorders of the frontotemporal lobar degeneration-amyotrophic lateral sclerosis spectrum: a gene identification study The Lancet Neurology *11*, 54-65.

Gistelinck, M., Lambert, J.C., Callaerts, P., Dermaut, B., and Dourlen, P. (2012). *Drosophila* Models of Tauopathies: What have we learned? . International Jounral of Alzheimer's Disease.
Herranz-Martin, S., Chandran, J., Lewis, K., and Azzouz, M. (2017). Viral delivery of C9orf72 hexanucleotide repeat expansions in mice leads to repeat-length-dependent neuropathology and behavioural deficits. Disease models and mechanisms *7*, 859-868.
Hogan, D.B., Jette, N., Fiest, K.M., Roberts, J.I., Pearson, D., Smith, E.E., Roach, P., Kirk, A., Pringsheim, T., and Maxwell, C.J. (2002). The prevalence of Frontotemporal Dementia. Neurology *58*, 1615-1621. 10.1212/wnl.58.11.1615
I

Mizielinska, S., S. Gronke, T. Niccoli, C. E. Ridler, E. L. Clayton, A. Devoy, T. Moens, F. E. Norona, I. O. Woollacott, J. Pietrzyk, K. Cleverley, A. J. Nicoll, S. Pickering-Brown, J. Dols, M. Cabecinha, O. Hendrich, P. Fratta, E. M. Fisher, L. Partridge and A. M. Isaacs (2014). "C9orf72 repeat expansions cause neurodegeneration in Drosophila through arginine-rich proteins." Science **345**(6201): 1192-1194.
Jiang, J., Zhu, Q., Gendron, T.F., Saberia, S., McAlonis, M., and Lagier-Tourenne, C. (2016). Gain of Toxicity from ALS/FTD-Linked Repeat Expansions in C9ORF72 Is Alleviated by Antisense Oligonucleotides Targeting GGGGCC-Containing RNAsJie. Neuron *90* 535-550.
Koppers, M., Blokhuis, A.M., and Pasterkamp, R.J. (2015). C9orf72 ablation in mice does not cause motor neuron degeneration or motor deficits. Annals of neurology, 426-438.
Lehmann, M., Rohrer, J.D., Clarkson, M.J., Ridgway, G.R., Scahill, R.I., Modat, M., Warren, J.D., Ourselin, S., Barnes, J., Rossor, M.N., and Fox, N.C. (2010). Reduced cortical thickness in the posterior cingulate gyrus is characteristic of both typical and atypical Alzheimer's disease Journal of Alzheimer's Disease *20*, 587-598.
Lewis, S.A., Negelspach, D.C., Cowen, S.L., and Fernandez, F. (2017). Spontaneous alteration: A potential gateway to spatial working memory in *Drosophila*. Neurobiology of Learning and Memory *142*, 230-235.
Liu, Y., Pattamatta, A., Zu, T., Yachnis, A.T., and Ranum, L.P.W. (2016). C9orf72 BAC Mouse Model with Motor Deficits and Neurodegenerative Features of ALS/FTD Neuron 521-534.
Mackenzie, M.D.-H.I.R., Boeve, B.F., Boxer, A.L., NiCole, M.B.N.J.R.A.M.N., Finch, A., Flynn, H., Adamson, J., and Rademakers, N.K.R. (2011). Expanded GGGGCC hexanucleotide repeat in noncoding region of C9ORF72 causes chromosome 9p-linked FTD and ALS Neuron *72*, 245-256. 10.1016/j.neuron.2011.09.011.
Mahoney, C.J., Beck, J., Rohrer, J.D., Lashley, T., Mok, K., Shakespeare, T., Yeatman, T., Warrington, E.K., Schott, J.M., Fox, N.C., et al. (2012). Frontotemporal dementia with the C9ORF72 hexanucleotide repeat expansion: clinical, neuroanatomical and neuropathological features Brain *135*, 736-750.
McKhann, G.M., Albert, M.S., Grossman, M., Miller, B., Dickson, D., and Trojanowski, J.Q. (2001). Clinical and pathological diagnosis of frontotemporal dementia: report of the Work Group on Frontoemporal Dementia and Pick's Disease. Archives of Neurology *58*, 1803-1809. 10.1001/archneur.58.11.1803.
Neary, D., Snowden, J.S., Gustafson, L., Passant, U., Stuss, D., Black, S., Freedman, M., Kertesz, A., Robert, P.H., Albert, M., et al. (1998). Frontotemporal lobar degeneration: a consensus on clinical diagnostic criteria Neurology *51*, 1546-1554. 10.1212/wnl.51.6.1546.

Pennington, C., Hodges, J.R., and Hornberger, M. (2011). Neural Correlates of Episodic Memory in Behavioral Variant Frontotemporal Dementia. Journal of Alzheimer's Disease *24* (*261-268*). 10.3233/JAD-2010-1016688.
Peters, O.M., Cabrera, G.T., Tran, H., and Jr, R.H.B. (2015). Human C9ORF72 Hexanucleotide Expansion Reproduces RNA Foci and Dipeptide Repeat Proteins but Not Neurodegeneration in BAC Transgenic Mice. Neuron *88*, 902-909.
Pitman, J.L., McGill, J.J., Keegan, K.P., and Allada, R. (2006). A dynamic role for the mushroom bodies in promoting sleep in *Drosophila*. Nature Communications *44*. 10.1038/nature04739.
Rascovsky, K., Hodges, J.R., Knopman, D., Mendez, M.F., Kramer, J.H., Neuhaus, J., van Swieten, J.C., Seelaar, H., Dopper, E.G., Onyike, C.U., et al. (2011a). Sensitivity of revised diagnostic criteria for the

behavioural variant of frontotemporal dementia. Brain a journal of neurology *134*, 2456-2477. 10.1093/brain/awr179
Rascovsky, K., Hodges, J.R., and Miller, B.L. (2011b). Sensitivity of Revised diagnostic criteria for the behavioural variant of frontotemporal dementia. Brain *134*, 2456-2477.
Renton, A.E., Majounie, E., Sanchez, A.W.J.S., Rollinson, S., and Gibbs, J.R. (2011). A hexanucleotide repeat expansion in C9orf72 is the cause of chromosome 9p21-linked ALS-FTD. Neuron. 10.1016/j.neuron.2011.09.010.
Rohrer, J.D., Guerreiro, M.R., and Rossor, M.M.N. (2009). The heritability and genetics of frontotemporal lobar degenration. Neurology *73*, 1451-1456.
Seltman, R.E., and Matthews, B.R. (2012). Frontotemporal lobar degeneration: epidemiology, pathology, diagnosis and management CNS Drugs *26*, 841-870.
Shao, Q., Liang, C., Chang, Q., Zhang, W., and Chen, J.-F. (2019). C9orf72 deficiency promotes motor deficits of a C9ALS/FTD mouse model in a dose-dependent manner. Acta Neuropathologica *7*.
Shaw, J.C.-K.P.J., and Kirby, J. (2014). The widening spectrum of C9orf72-related disease;genotype/phenotype correlations and potential modifiers of clinical phenotype. Acta Neuropathologica *127*.
Shaw, P.J., Cirelli, C., Greenspan, R.J., and Tononi, G. (2000). Correlates of sleep and waking in Drosophila melanogaster Science 10.1126/science.287.5459.1834.
Simone, R., Balendra, R., Moens, T.G., Preza, E., Wilson, K.M., Heslegrave, A., Woodling, N.S., Niccoli, T., Gilbert-Jaramillo, J., Abdelkarim, S., et al. (2018). G-quadruplex-binding small molecules ameliorate C9orf72 FTD/ALS pathology in vitro and in vivo. EMBO molecular medicine *10*, 22-31.
Smith, B.N., and Shaw, S.N.C.E. (2013). The C9ORF72 expansion mutation is a common cause of ALS+/−FTD in Europe and has a single founder. Nature european journal of human genetics *21*, 102-108.
Therrien, M., Rouleau, G.A., Dion, P.A., and Parker, J.A. (2013). Deletion of C9ORF72 results in motor neuron degeneration and stress sensitivity in C. elegans PLoS One *12*.
Todd, T., McEachin, Z.T., Bassel, G.J., and Petrucelli, L. (2020). Hexanucleotide Repeat Expansions in c9FTD/ALS and SCA36 Confer Selective Patterns of Neurodegeneration In Vivo. Cell Reports.

Trojanowski, J.Q., and Dickson, D. (2001). Update on the neuropathological diagnosis of frontotemporal dementias Journal of Neuropathology and experimental neurology *60*, 1123-1126.
Turner, G.C., Bazhenov, M., and Laurent, G. (2008). Olfactory representations by *Drosophila* mushroom body neurons. Journal of neurophysiology *99*, 734-746. 10.1152/jn.01283.2007
van der Zee, J., Gijselinck, I., Dillen, L., Van Langenhove, T., Theuns, J., Engelborghs, S., Philtjens, S., Vandenbulcke, M., Sleegers, K., Sieben, A., et al. (2013). A pan-European study of the C9orf72 repeat associated with FTLD: geographic prevalence, genomic instability, and intermediate repeats. Human mutation. 10.1002/humu.22244.
Warren, J.D. (2013). Frontotemporal Dementia Biomedical Journal

Wood, E.M., Falcone, D., and Grossman, M. (2013). Development and Validation of Pedigree Classification Criteria for Frontotemporal Lobar Degeneration. JAMA Neurology *70*, 1411-1417.
Young, A.L., Bocchetta, M., Russell, L.L., Convery, R.S., Peakman, G., Todd, E., Cash, D.M., Greaves, C.V., van Swieten, J., Jiskoot, L., et al. (2021).
Characterizing the Clinical Features and Atrophy Patterns of MAPT-Related Frontotemporal Dementia With Disease Progression Modeling Neurology *97*, 941-952.
Z, S. (2018).
Mechanisms Associated wit h TDP -43 Neurotoxicity in ALS/FTL. Advanced Neurbiology.
Zhu, Q., Jiang, J., Gendron, T.F., and Lagier-Tourenne, C. (2020).
Reduced C9ORF72 function exacerbates gain of toxicity from ALS/FTD-causing repeat expansion in C9orf72. Nature Neuroscience, 615-624.
Zhu, Y.S.R.Q.X.L.Y.C.S.G.F.K.L.L.Y. (2020). Social Attraction in *Drosophila* is regulated by the mushroom body and serotonergic system. Nature Communications *11*.